Hydride-Rhodium(III)-N-Heterocyclic Carbene Catalyst for Tandem Alkylation/Alkenylation via C-H Activation

Ramón Azpíroz,[†] Andrea Di Giuseppe,[†] Asier Urriolabeitia,[§] Vincenzo Passarelli,[‡,†] Victor Polo,[§] Jesús J. Pérez-Torrente,[†] Luis A. Oro[†], and Ricardo Castarlenas,*[,†]

[†]Departamento de Química Inorgánica – Instituto de Síntesis Química y Catálisis Homogénea-ISQCH, Universidad de Zaragoza – CSIC, C/ Pedro Cerbuna 12, 50009 Zaragoza, Spain

[‡]Centro Universitario de la Defensa, Ctra Huesca S/N 50090 Zaragoza, Spain

[§]Departamento de Química Física, Universidad de Zaragoza, C/ Pedro Cerbuna 12, 50009 Zaragoza, Spain

KEYWORDS C-H activation, C-C coupling, Hydroarylation, N-heterocyclic carbene, Rhodium

ABSTRACT: The unsaturated hydride complex RhClH{*k*-N,*k*-C-($C_{11}H_8N$)}(IPr) {IPr = 1,3-bis-(2,6-diisopropylphenyl)imidazolin-2-carbene} (**2**) has been prepared via C-H activation of 2-phenylpyridine and fully characterized by spectroscopic methods and X-ray diffraction analysis. Complex **2** efficiently catalyzes the isomerization of terminal and internal olefins under mild conditions to give preferentially the *E* regioisomers. Complex **2** also catalyzes the hydroarylation of terminal olefins with 2-phenylpyridine to yield selectively mono-*ortho*-alkylated derivatives. Tandem isomerization-alkylation processes were observed for internal olefins. In contrast to olefins, double alkenylation is operative for internal alkynes. The marked complementary reactivity of olefins and alkynes toward hydroarylation with 2-phenylpyridine allows for a tandem alkylation/alkenylation transformation to yield substituted styrenes. These heterobiaryl compounds exhibit axial chirality which have been experimentally calculated and corroborated by DFT calculations. A catalytic cycle for hydroarylation reactions has been proposed based on the identification of key reaction intermediates and H/D exchange experiments. The reaction seems to proceed by initial C-H activation of 2-phenylpyridine, subsequent insertion of alkene or alkyne, and reductive elimination steps. DFT calculations shows that reductive elimination is the rate determining step for alkene hydroarylation whereas migratory insertion is the highest barrier for alkyne hydroarylation.

INTRODUCTION

Transition metal mediated C-H activation is a powerful and versatile methodology for the preparation of high added value organic scaffolds in a selective and atom-economical manner.[1] Precise control over reactivity of the metallic center is of paramount importance in order to construct elaborated architectures from simple starting materials. Particularly, π-conjugated alkenyl-arenes (or styrenes) are attractive synthetic targets due to its relevant applications in medicinal chemistry and functional materials.[2] One of the most reliable catalytic methods that has remarkably contributed to this field is the Mirozoki-Heck approach.[3] However, the requisite of a preactivated arene constitutes an important drawback (Scheme 1). Alternatively, many research efforts have been directed to the oxidative coupling of arenes with alkenes after the pioneering work by Fujiwara and Moritani with palladium catalysts.[4] In spite of these remarkable advances,[5] selectivity issues are still challenging. Another completely different synthetic access to styrenes is the addition of an aromatic ring across a carbon-carbon triple bond, namely hydroarylation of alkynes.[6] Interestingly, simple unbiased arenes can be engaged in this total atom-economy approach. Depending on the substrates and the metallic fragment, activation of the alkyne can occur previously to electrophilic Friedel-Crafts attack of the aryl group, thereby resulting in *trans*-addition products.[7] However, this methodology is generally limited to electron-rich arenes, heteroarenes or intramolecular processes. An alternative pathway entails an initial C-H activation of the arene followed by a C-C coupling with the alkyne.[8] The process can occur via a metal-hydride intermediate[8a-b] or, alternatively, by a redox-neutral base-mediated[8d] or ligand-to-ligand proton transfer mechanism.[8e] In these cases, in contrast to the Friedel-Crafts pathway, acidic electron-deficient arenes are preferred.

A foremost milestone in alkyne hydroarylation was the introduction of a directing group in the arene moiety. This step-forward expanded the range for operative aromatic groups and unsaturated substrates, as demonstrated by the seminal work of Murai's group[9] in ruthenium-catalyzed hydroarylation of olefins[9a] and alkynes.[9b] Efficient catalysts do not limit to ruthenium-based examples,[10] but other transition metal catalysts based on iridium,[11] cobalt,[12] manganese,[13] and particularly rhodium,[14] have been involved in directing group-promoted alkyne hydroarylation. Generally, the reaction can proceed by two main distinct routes: *i*) the classical Murai´s pathway that entails the formation of a metal-hydride intermediate via oxidative addition,[9a-b,10a,c,k,11c,12b,14a-g] and *ii*) a nonoxidative electrophilic or base-promoted aromatic C-H activation.[10b,d-j,l,11a,12c-f,13,14i] The participation of a metal-hydride species in the former mechanism accelerates the insertion step whereas higher selectivity has been claimed in the case of nonoxidative processes. Even though the directing group facilitates the C-H activation, the presence of free *ortho* positions on the aromatic

ring requires the control of the reactivity in either one[10b,d,f,g,i,k,l,11b,c,12a-d,f,13,14b,c,e,g,j] or both reaction sites,[10h,j,l,11b,12a,d,e,14a,b,d,f,h] in addition to the regioselectivity issues for unsymmetrical alkynes. Consequently, more research efforts still have to be done with the aim of developing more efficient catalytic systems.

Scheme 1. Transition Metal-Mediated Preparation of Styrenes

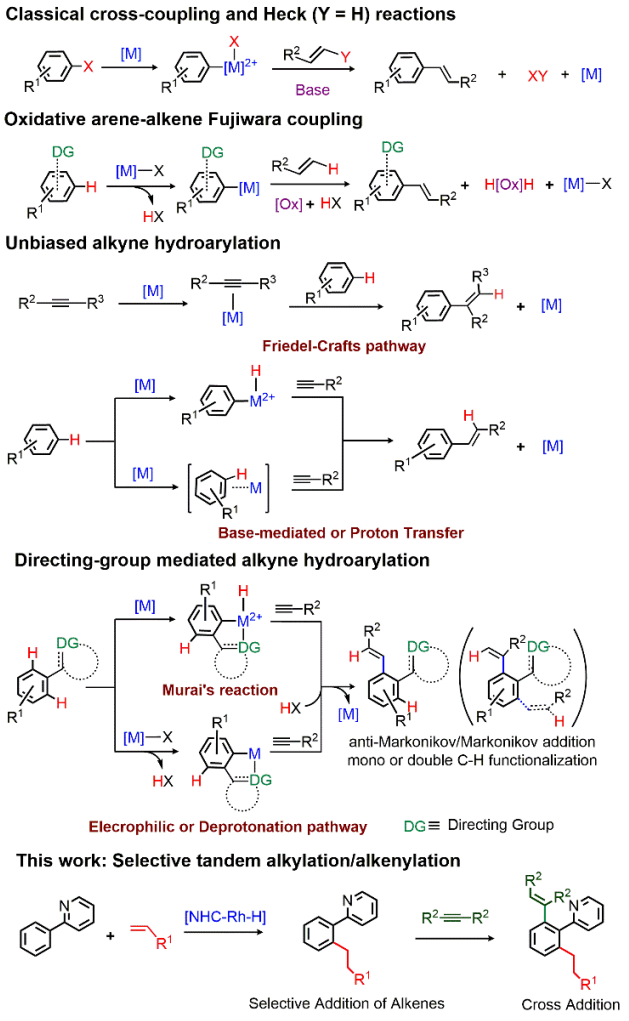

The advent of N-heterocyclic carbenes (NHCs) as ligands for transition metal complexes has revolutionized the field of homogeneous catalysis,[15] with important significance in C-H activation.[16] As very powerful electron-donating ligands, NHCs favor oxidative addition processes. In addition, their generally high steric hindrance allows for a control over selectivity. Being aware of this fact, our research group has developed in recent years a variety of NHC-based rhodium catalysts active in C-H activation.[17] Particularly, dinuclear compounds of type [Rh(μ-Cl)(NHC)(η^2-olefin)]$_2$, proved to be valuable starting materials for the preparation of mononuclear complexes RhCl(NHC)(η^2-olefin)(L) by simple bridge-cleavage with a nucleophilic ligand.[18] These derivatives exhibited excellent activities and selectivities in catalytic alkyne homo-[17c] and cross-dimerization,[17d] as well as hydroalkenylation of N-vinylpyrazoles,[17f] 2-thienylpyridine,[17g] and 2-vinylazines[17b,h] to produce valuable N-bridge heterocycles. In the course of the research, we have observed that the presence of a nitrogen-directing group facilitates the formation of metal-hydride intermediate species. Notably, besides the pioneering work of Murai's group with $RuH_2(CO)(PPh_3)_2$[9] and that of the Prof. Yi and coworkers using the cationic complex $[(C_6H_6)RuH(CO)(PCy_3)]BF_4$,[19] metal-hydride derivatives have been only scarcely introduced as pre-synthesized catalytic precursors in C-H activation process.[10a,17g,20] This gap might seem surprising due to the inherent advantage of using species directly involved in the catalytic cycle as catalyst precursors, thus avoiding preactivation steps. Moreover, metal-hydrides are also known to be efficient catalysts for olefin isomerization[21] which open the way to the development of tandem catalytic processes.[22] Herein, we report on the N-directed hydroarylation of unsaturated substrates catalyzed by a new hydride-rhodium-NHC compound. The high selectivity towards the mono-hydroarylated product using olefins, allows for the controlled preparation of a range of substituted styrenes by subsequent alkenylation of these intermediate derivatives with internal alkynes. The hydride precursor is also efficient in olefin isomerization and tandem processes involving hydroarylation reactions. In addition, the proposed has been investigated by theoretical calculations at DFT level.

RESULTS AND DISCUSSION

The ability of [Rh(μ-Cl)(IPr)(η^2-coe)]$_2$ (**1**) {IPr = 1,3-bis-(2,6-diisopropylphenyl)imidazolin-2-carbene} to undergo C-H activation of arylpyridines has been evidenced by the reaction of **1** with 2-phenylpyridine. After 2 h at 80 ºC, the unsaturated hydride complex RhClH{κ-N,κ-C-($C_{11}H_8N$)}(IPr) (**2**) was obtained, which was isolated as a yellow solid in 87% yield (Scheme 2). The presence of a hydride ligand in **2** is corroborated by a shielded doublet at δ -24.67 ppm in the ^{1}H NMR spectrum at -30 ºC. The high $J_{H\text{-}Rh}$ (50.2 Hz) points to a square-pyramidal structure with the hydride located at the apical position.[17a] Moreover, the ^{13}C{^{1}H}-APT NMR spectrum displays two doublets at δ 185.7 ($J_{C\text{-}Rh}$ = 57.0 Hz) and 163.9 ($J_{C\text{-}Rh}$ = 32.0 Hz) ppm, corresponding to the carbene and the *ortho*-metalated carbon atoms, respectively. Metal-NHC complexes bearing activated phenylpyridine are well-known, but the disposition of the quelate ligand does not follow a clear trend. In fact, coordination of the pyridine moiety *cis*[23] or *trans*[24] to the carbene depends on subtle stereoelectronic effects within the metal environment. Moreover, isolated complexes containing hydride and ortho-metalated phenylpyridine ligands are very scarce,[25] since usually they are transient species that easily undergo reductive elimination. It is worthy to note that complex **2** has been previuosly *in-situ* detected as an intermediate in borylation reactions.[25b]

Scheme 2. Preparation of RhClH{κ-N,κ-C-($C_{11}H_8N$)}(IPr) by C-H Activation of 2-Phenylpyridine

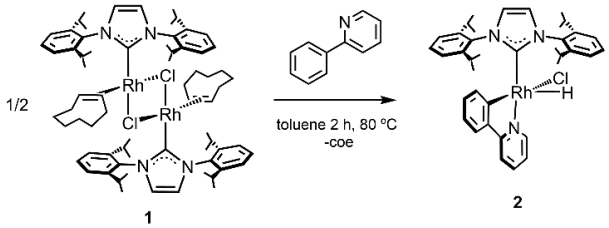

In order to establish the stereochemistry of **2**, an X-ray structural analysis has been performed. (Figure 1). The asymmetric unit of **2** contains two crystallographically independent molecules (see Figure S1 in Supporting Information) showing very similar angles and bond lengths, thus only one of the two

complexes is discussed herein. The metal center exhibits a distorted square pyramid coordination polyhedron (τ 0.17)[26] in which the hydride ligand occupies the apical position and the carbene carbon atom C(1) and the chlorine atom two equatorial *cis* positions. The ortho-metalated 2–phenyl pyridine occupies the two remaining equatorial *cis* positions with the nitrogen atom N(30) *trans* to the IPr carbon atom [N(30)–Rh(1)–C(1) 177.81(7)°]. The two aromatic rings are almost coplanar [N(30)–C(31)–C(36)–C(37) 3.98(29)°] with a C(31)–C(36) bond length of 1.462(3) Å,[27] nicely fitting in with a Csp^2–Csp^2 single bond. The pitch (θ) and the yaw (ψ) angles[17f] of the NHC moiety are close to cero indicating an almost ideal arrangement of the NHC ring with respect to the Rh(1)–C(1) bond. Further, as a consequence of the chelate (κ-*N*,κ-*C*) coordination mode of the metallated phenylpyridine the yaw angles of the pyridyl and the phenyl moieties have similar values but opposite signs (pyridyl –5.6°; phenyl, +7.5°). On the other hand, probably as a consequence of the small torsion angle N(30)–C(31)–C(36)–C(37) [3.98(29)°], small pitch angles are observed for the pyridyl (0.3°) and the phenyl (4.8°) moieties. Finally, it is worth a mention that, to the best of our knowledge, **2** is the first structurally characterized Rh–NHC–hydride complex resulting from a C–H activation of 2–phenylpyridine.

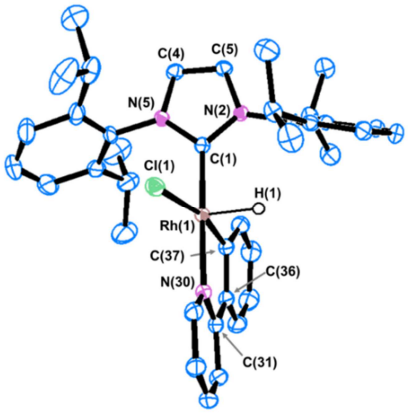

Figure 1. ORTEP view of RhClH{κ-*N*,κ-*C*–($C_{11}H_8N$)}(IPr) (**2**) with the thermal elipsoids at 50 %. Only one complex of the asymmetric moiety is shown and most hydrogen atoms have been omitted for clarity. Selected bond lengths (Å) and angles (°) are: Rh(1)–C(1) 1.9994(19); Rh(1)–Cl(1) 2.4277(5); Rh(1)–N(30) 2.1020(17); Rh(1)–C(37) 1.995(2); C(36)-C(31) 1.462(3); C(1)–Rh(1)–N(30) 177.81(7); C(37)–Rh(1)–Cl(1) 167.87(6); C(1)–Rh(1)–Cl(1) 89.92(6); C(37)–Rh(1)–N(30) 80.29(8); C(37)–Rh(1)–H(1) 79.5(11); C(1)–Rh(1)–H(1) 85.8(11); N(30)–Rh(1)–H(1) 93.6(11); Cl(1)–Rh(1)–H(1) 110.7(11), C(37)–C(36)–C(31)–N(30) 3.98(29). Pitch (θ) and yaw (ψ) angles (°) are: NHC, θ 2.0, ψ –1.7; pyridyl, θ 0.3, ψ –5.6; phenyl, θ 4.8, ψ 7.5.

Catalytic Activity in Olefin Isomerization. The particular structure of hydride complex **2** prompted us to study its performance in olefin isomerization reactions.[21] Catalytic tests with 5 mol% loading of **2** in C_6D_6 at room temperature showed excellent activity for the isomerization of terminal and *Z*-olefins to yield *E*-alkenes with high selectivity (Scheme 3, Table 1). Short times were needed to efficiently isomerize allylbenzene or 1-octene with very high *E*/*Z* selectivity (entry 1-2). The terminal olefin 4-phenyl-1-butene was isomerized into 4-phenyl-2-butene in 20 min at room temperature (entry 3), which smoothly evolved further into 1-phenyl-1-butene (50% conversion after 12 h at room temperature). Direct chain-walking isomerization[22e] of 4-phenyl-1-butene to the conjugated olefin was attained at 80 ºC for 1 h with complete selectivity for the *E*-isomer (entry 4). 1,5-Hexadiene was also susceptible of isomerization to yield 2,4-hexadiene, showing a thermodynamic *E*,*E*/*E*,*Z* ratio of 81/19 (entry 5). Interestingly, the formation of 1,4-hexadiene resulting from the isomerization of only one double bond was observed at the early stage of the reaction. The reactivity of allyl butyl ether was somewhat different. Terminal-to-internal olefin isomerization was almost complete in 25 min with 70% *E*-selectivity (entry 6). However, the amount of *Z*-isomer smoothly increased with time reaching a thermodynamic equilibrium with *E*/*Z* ratio of 45/55 (entry 7, see Fig S2 in Supporting Information). An internal olefin such as *cis*-stilbene was isomerized to *trans*-stilbene in only 5 min with 99% selectivity (entry 8). Rather surprisingly, isomerization of diethyl 2,2-diallylmalonate did not take place at room temperature (entry 9). However, heating the sample at 80 ºC for 5 min resulted in the diastereoselective formation of the exocyclic alkene derivative diethyl 3-methyl-4-methylenecyclopentane-1,1-dicarboxylate.[28]

Scheme 3. Mechanism for Olefin Isomerization Catalyzed by 2

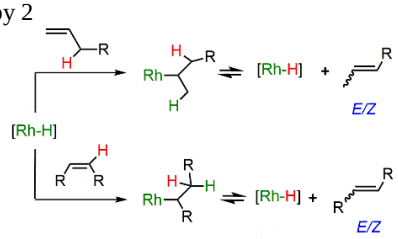

Table 1. Olefin Isomerization Promoted by 2[a]

Entry[a]	Olefin	Product	t(min)	Conv (%)	*E*/*Z*
1			30	99	98/2
2			15	98	99/1
3			20	99	86/14
4			60[b]	99	99/1
5			180	99	81/19
6	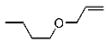	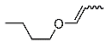	25	98	70/30
7	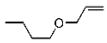	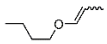	60	99	45/55
8		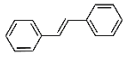	5	--	99/1
9	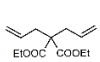		5[b]	99	--

[a]0.5 mL of C_6D_6, 5 mol% of complex **2**, [alkene] = 0.4 M at room temperature. [b]80°C. [c]Isomerization not detected.

The assumed alkene isomerization mechanism entails the insertion of the olefin in the rhodium-hydride bond (Scheme 3). Accordingly, the hydride signal of **2** disappeared from the ^{1}H NMR spectrum just after addition of a terminal olefin. However, that resonance emerges again at high conversions without a detrimental influence on the catalytic activity in the case of chain walking isomerization (entry 4). This fact indicates that, in spite of the high steric hindrance of the IPr ligand, insertion of internal olefins occurs but the Rh-alkyl in-

termediate formed is in equilibrium with the more stable Rh-hydride. The observed selectivity to *E*-olefins for catalyst **2** points to a kinetic origin, likely due to a favored *β*-elimination step,[17a,e] since increasing of time or temperature results in an increment of *Z*-amount in accordance to thermodynamic equilibrium.

Alkene Hydroarylation. The notable catalytic activity of complex **2** for olefin isomerization under mild conditions arises from the easy insertion of alkenes into the Rh-H bond. This fact evidences its potential as catalyst for carbon-carbon coupling reactions. Accordingly, the hydride complex **2** has been revealed as a valuable catalyst for the hydroarylation of terminal olefins with 2-phenylpyridine (Scheme 4).[29] The reactions were carried out in sealed NMR tubes with 5 mol% of **2** using C_6D_6 as solvent at 90 ºC and monitored by ^{1}H NMR.

Scheme 4. Hydroarylation of Alkenes with 2-Phenylpyridine

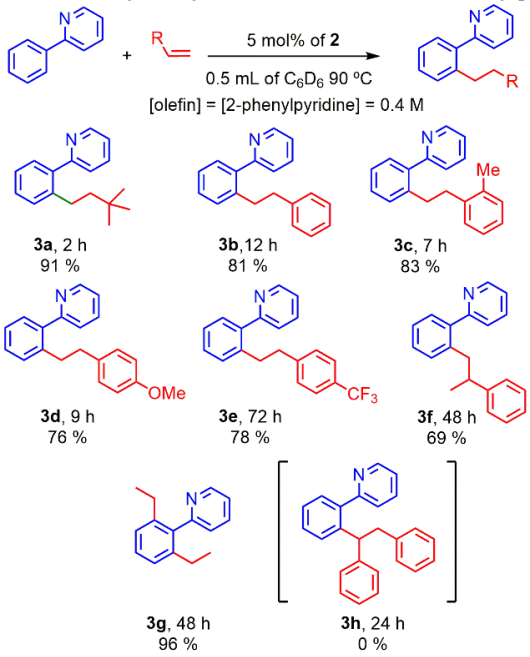

The selective alkylation of only one of the *ortho* positions of 2-phenylpyridine was observed, except for ethylene. Linear 2-(2-alkylphenyl)pyridine derivatives resulting from anti-Markovnikov hydroarylation were exclusively isolated with good to high yields. Furthermore, the reaction worked well with both aryl and aliphatic alkenes. The hydroarylation of 2-phenylpyridine with 3,3-dimethyl-1-butene was complete in 2 h affording **3a** with 91% isolated yield whereas styrene needed 12 h to be transformed into **3b**. The catalytic activity is quite sensitive to the electronic effects on the aromatic ring of the olefin. Thus, electron-donating groups increased the hydroarylation rate (**3c-d**), whereas a reduction of the catalytic activity was observed for electron-releasing groups (**3e**). The introduction of a substituent in the α position also resulted in a drastic drop in activity (**3f**, 48 h, 69% isolated yield), whereas *cis*-stilbene did not react at all, likely due to steric effects. Accordingly, reaction with ethylene (2 bar for 48 h) resulted in the double alkylated product **3g**. It is interesting to note that the dimer **1**, precursor of **2**, is a poor hydroarylation catalyst, indicating that *catalyst preformation is essential for efficient catalysis*.

Terminal olefins susceptible to isomerization exhibited distinct reactivity. For example, 1-octene, 3-phenyl-1-propene or 4-phenyl-1-butene quickly isomerized in the presence of **2** to the corresponding internal olefin under the hydroarylation catalytic conditions. In spite of the lack of reactivity observed for an internal olefin such as *cis*-stilbene (Scheme 4), C-C coupling between 2-phenylpyridine and these olefins proceeded efficiently (Scheme 5). However, the outcome of the reaction was not the expected branched alkyl derivative resulting from the coupling of the internal olefin, but the linear one arising from the terminal alkene was obtained instead. Indeed, the same linear alkyl derivative was formed starting from 1-octene, 2-*E*-octene or 2-*Z*-octene. These tandem isomerization-hydroarylation processes are directed by the interplay of thermodynamic and kinetic factors. Thus, the isomerization of terminal to internal alkene is thermodynamically preferred, whereas the coupling of terminal olefin with 2-phenylpyridine is kinetically favored.[22] Another interesting tandem process is the cyclization-hydroarylation of the terminal diene 2,2-diallylmalonate with 2-phenylpyridine to afford **3l** in 67% isolated yield.

Scheme 5. Tadem Isomerization-Hydroarylation and Cyclization-Hydroarylation Reactions

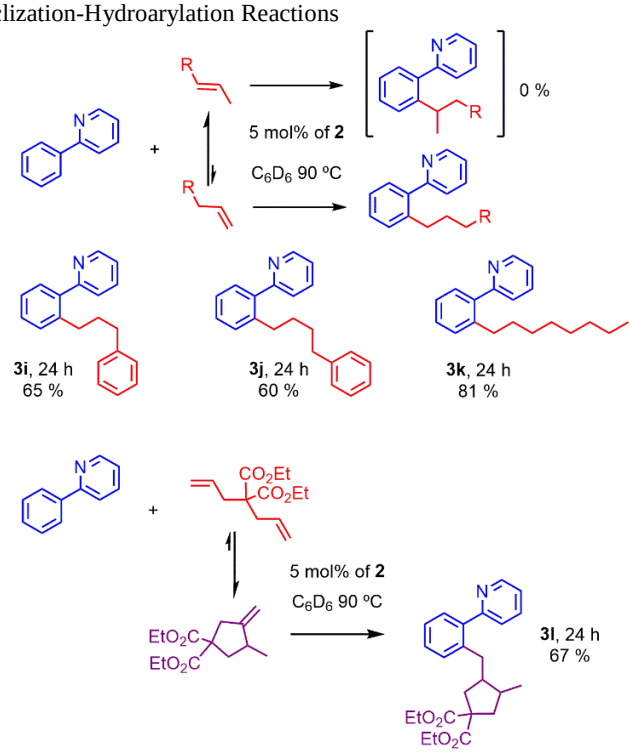

Alkyne Hydroarylation. Complex **2** efficiently catalyzed the hydroarylation of internal alkynes with 2-phenylpyridine. In contrast to olefins, the double alkenylation of 2-phenylperydine to yield 2-(2,6-bis-alkenyl-phenyl)pyridine derivatives was exclusively observed (Scheme 6). The stereochemistry of the products was confirmed by ^{1}H-NOESY NMR experiments. The *E-E* isomer **4a** was exclusively formed as a result of tandem *syn* hydroarylation of two molecules of 4-octyne. Alternatively, the initially formed *E-E* product **4b** from diphenylacetylene underwent an isomerization process on one of the *ortho*-alkenyl groups to afford the *E-Z* mixed 2-(2,6-bis-alkenyl-phenyl)pyridine **4b´**, which was the sole isomer isolated after column chromatography (88% yield). Unfortunately, the hydroarylation of terminal alkynes such as phenylacetylene, benzylacetylene or 1-hexyne was unsuccessful due to competitive dimerization, cyclotrimerization and polymerization reactions.

Scheme 6. Hydroarylation of Internal Alkynes with 2-Phenylpyridine

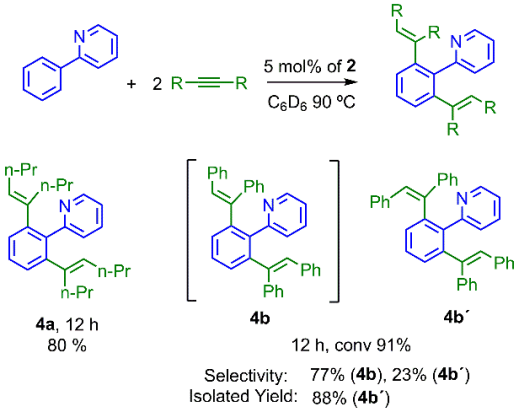

Tandem Alkylation/Alkenylation. The marked complementary reactivity of alkenes and alkynes in hydroarylation reactions with 2-phenylpyridine promoted by **2** prompted us to combine these two reactions in a tandem process in order to prepare 2-(2-alkyl-6-alkenyl-phenyl)pyridine derivatives with good to high yields (Scheme 7).[30] In a preliminary test, styrene, diphenylacetylene and 2-phenylpyridine were mixed in the presence of **2**. Unfortunately, only the alkyne hydroarylation products **4b** and **4b'** were obtained, indicating that alkynes react faster than olefins, thus inhibiting the tandem process. Therefore, it was necessary to perform the reaction in two steps. Firstly, the alkene hydroarylation to form the monoalkylated arylpyridine derivatives, and subsequently the hydroarylation of an internal alkyne in the same reactor to synthesize the unsymmetrical alkyl-alkenyl di-substituted phenylpyridine derivatives 2-(2-alkyl-6-alkenyl-phenyl)pyridine **5-6**. A comparative study of the rate of the catalytic reactions using styrene and diphenylacetylene as substrates showed that the double alkenylation of 2-phenylpyridine is faster than olefin hydroarylation, as expected from the observed catalytic outcome (see Fig S3 in Supporting Information). However, alkenylation of alkylated-phenylpyridine has an intermediate rate. This fact points to an electronic effect playing a role in the second hydroarylation step, since alkenyl-substitution accelerates the reaction over alkyl-funcionalization.

The synthetic scope of this tandem process was analyzed by using a range of alkyl and aryl terminal olefins and diphenylacetylene or 4-octyne as internal alkynes (Scheme 7). As a general trend, diphenylacetylene reacted faster than 4-octyne (**5** *vs* **6**). Indeed, the presence of a substituent on the alkylated phenylpyridine also influences the catalytic activity with a similar trend to that observed in olefin hydroarylation. Thus, hydroarylation of diphenylacetylene with 2-(2-neopentylphenyl)pyridine, **3a**, afforded **5a** in 71% yield after 4 h, whereas 2-{2-(2-phenylethyl)phenyl}pyridine, **3b**, gave **5b** in 81% yield after 7 h. Moreover, electron density on the aromatic ring of the pendant alkylic chain also affects the performance of the catalyst. As observed for the olefin hydroarylation, an electron-donating group increases the catalytic activity (**5d**), while it is reduced with an electron-withdrawing substituent (**5e**). The reaction involving compound **3f** containing a methyl group on the aliphatic chain required a higher catalyst loading (10 mol%) and high temperature (120 ºC) to afford **5f** in 65% yield. Interestingly, the same trends were observed in the tandem alkene/alkyne hydroarylation reactions involving 4-octyne.

Scheme 7. Tandem Alkylation/Alkenylation of 2-Phenylpyridine with Olefins and Internal Alkynes

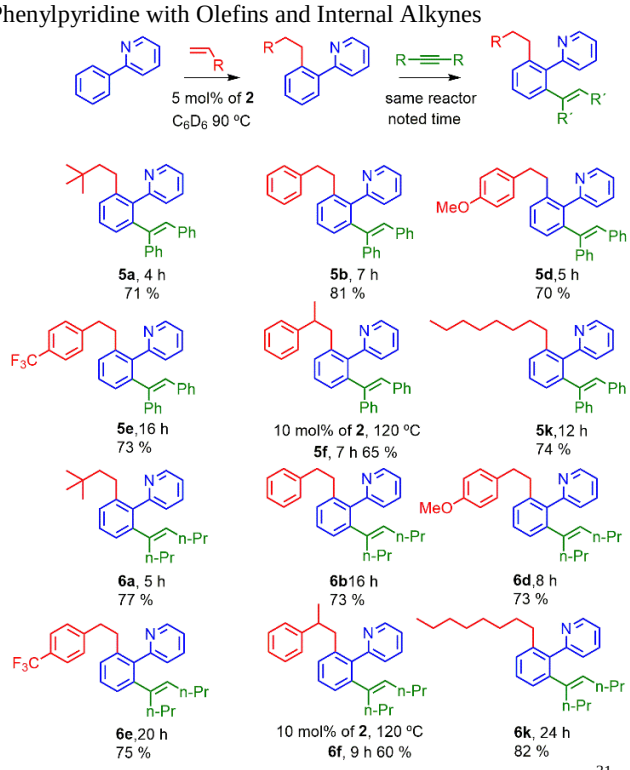

The heterobiaryl compounds **5-6** exhibit axial chirality.[31] Rotation around the biaryl axis is restricted in such derivatives, and depends on the nature of the substituent of the alkyl chain, as it becomes evident from the fluxional behavior observed in the ^{1}H NMR spectra. Thus, the coalescence peak observed at room temperature for the $>CH_2$ protons adjacent to the phenyl group of **5a** splits into two triplets at -40 ºC (Figure 2). Line-shape simulation using the gNMR modeling package and further Eyring analysis allow the calculation of the activation parameters for the rotation process that turn out to be ΔH = 12.8±1.1 kcal mol^{-1} and ΔS = 1.4±2.1 cal mol^{-1} K^{-1}. Moreover, the rotational process for **5a** was studied by DFT calculations (Figure 2, top right). the relaxed potential energy surface (PES) scan was performed by considering the N-C2-C7-C8 dihedral angle value. PES scan was carried out around the bond C2–C7 by changing the torsion angle in 10° steps from –180° to +180°. Energy barriers of 13.6 and 11.3 kcal mol^{-1} were calculated between the more stable perpendicular dispositions and the coplanar structures, which agrees with the experimental values.

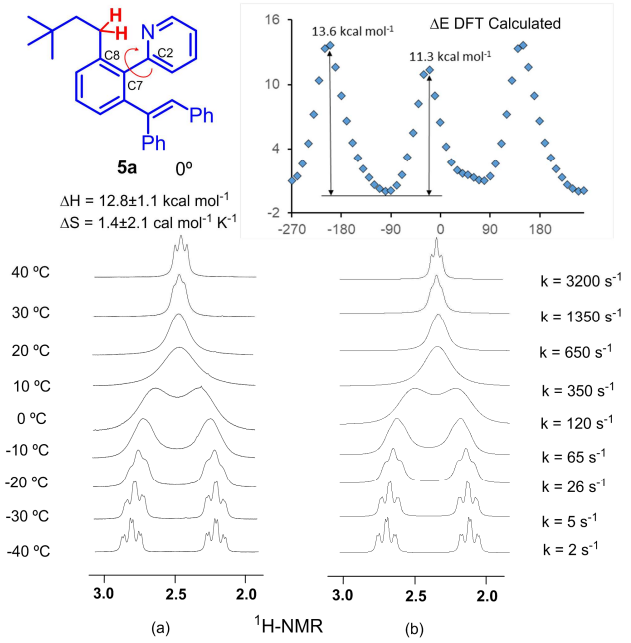

Figure 2. Variable temperature NMR spectra of **5a** in CD_2Cl_2 showing the coalescence of the two diastereotopic protons of the CH_2Ph fragment: experimental (bottom left) and calculated (bottom right). Potential energy surface scan for the rotation of the pyridine-phenyl axis (top right).

Mechanistic studies. In order to gain insight into the reaction mechanism, a series of stoichiometric reactions at low temperature were carried out (Scheme 8). A toluene-d_8 solution of **2** in a NMR Young-tube under 2 bar of ethylene at -30 °C afforded the Rh-ethyl complex RhCl(Et){κ-N,κ-C-($C_{11}H_8N$)}(IPr) (**7**) as a result of the insertion of ethylene into the Rh-H bond. A similar linear alkyl complex RhCl(C_2H_4Ph){κ-N,κ-C-($C_{11}H_8N$)}(IPr) (**8**) was obtained after treatment of **2** with styrene at -30 ºC, via anti-Markovnikov selective insertion. However, both alkyl complexes behave very differently at room temperature. The intermediate **7** in the presence of ethylene gas evolved to the formation of the reduced Rh^I-ethylene dimer [Rh(μ-Cl)(IPr)(η^2-C_2H_4)]$_2$ (**9**) and the coupled product 2-(2,6-diethylphenyl)pyridine **3g**. In contrast, no C-C coupling was observed when **8** was warmed to room temperature. Instead, an η^2-styrene complex RhCl(η^2-CH_2=CHPh)(κ-N,2-phenylpyridine)(IPr) (**10**) bearing a 2-phenylpyridine κ-*N* coordinated ligand was obtained via regeneration of **2** by β-hydride elimination and subsequent hydride-aryl reductive elimination. These results clearly demonstrated the reversibility of the C-H activation and migratory insertion processes. In contrast to the olefins, no reaction was observed after addition of diphenylacetylene to a solution of **2** at room temperature. However, after heating the sample at 80 ºC for one night, a mixture of **4b**, **4b'** and other unidentified compounds was obtained.

Scheme 8. Detected Intermediates for Olefin Hydroarylation Reaction

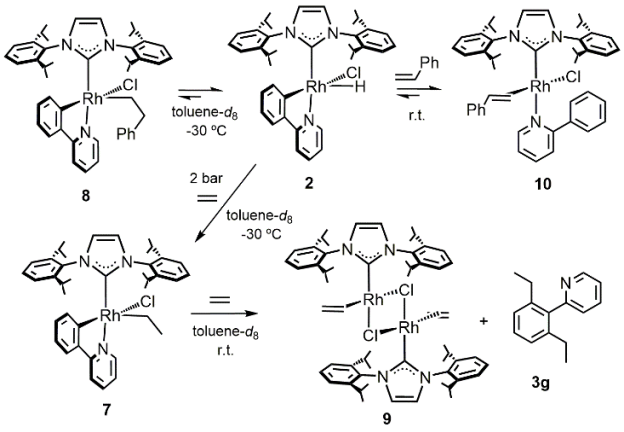

The NMR spectra of **7**, **8** and **10** are in agreement with proposed structures in Scheme 8. The presence of alkyl ligands in **7** and **8** is corroborated by the appearance in the ^{1}H NMR spectra of the signals corresponding to the diastereotopic methylene protons at δ 2.85 and 1.75 ppm for **7** and 2.94, 2.17, 1.74 and 1.68 ppm for **8**. Moreover, the $^{13}C\{^1H\}$-APT NMR spectra show three doublets for the corresponding Rh-C carbon atoms. The more deshielded signal appears at δ 181.5 (**7**) and 181.2 ppm (**8**), with Rh-C coupling around 60 Hz, corresponding to the carbene carbon atom. The *ortho*-metalated rhodium-aryl carbon atom resonates at 172.9 (**7**) and 172.4 ppm (**8**), displaying smaller $J_{C\text{-}Rh}$ values around 39 Hz. Finally, the Rh-alkyl carbon atoms are observed at 18.3 (d, $J_{C\text{-}Rh}$ = 32.4 Hz) and 23.4 ppm (d, $J_{C\text{-}Rh}$ = 34.3 Hz), for **7** and **8**, respectively. On the other hand, the ^{1}H NMR spectrum of complex **10** shows a set of signals at δ 4.55 (dd, $J_{H\text{-}H}$ = 12.3, 7.6 Hz, C<u>H</u>=CH_2), 2.24 (d, $J_{H\text{-}H}$ = 7.6 Hz, CH=C<u>H</u>$_2$) and 1.63 ppm (d, $J_{H\text{-}H}$ = 12.3 Hz, CH=C<u>H</u>$_2$), which confirms the coordination of styrene to the rhodium atom. The $^{13}C\{^1H\}$-APT NMR spectra of **10** also show three doublets, one for the Rh-C_{IPr} carbon atom (181.9, d, $J_{C\text{-}Rh}$ = 54.0 Hz) and two for the η^2-coordinated styrene at δ 54.1 ($J_{C\text{-}Rh}$ = 16.1 Hz, <u>C</u>H=CH_2) and 32.3 ($J_{C\text{-}Rh}$ = 15.6 Hz, CH=<u>C</u>H$_2$).

As we have shown, the catalytic activity of complex **2** is affected by equilibrium processes both in C-H activation as well as in insertion steps. To shed light on the hydroarylation mechanism deuterium-labeling experiments have been performed (Scheme 9). The catalytic H/D exchange on 2-phenylpyridine (0.18 mmol) with CD_3OD (0.5 mL) promoted by **2** (5 mol%) showed 73% of incorporation of deuterium atoms at both *ortho* positions of 2-phenylpyridine after 12 h at 80°C. Otherwise, treatment of 2-phenylpyridine with styrene-d_8 (0.18 mmol) in 0.5 mL of C_6D_6 in the presence of **2** (5 mol%) produced a H/D exchange between vinyl fragment of perdeuterated styrene (60, 58 and 54%) and both *ortho*-aryl protons of 2-phenylpyridine (60%) after 3 h at room temperature. Then, heating the sample for 12 h at 80 °C, resulted in the formation of the anti-Markovnikov 2-(2-phenethylphenyl)pyridine product, with both CH_2 groups (60 and 62%) and *ortho*-arene positions (57%) partially deuterated. The observed pattern for H/D exchange confirms the existence of equilibriums both on C-H activation and insertion steps of the catalytic cycle. In addition, the similar amount of deuterium incorporation at the α and β positions of styrene implies that Markovnikov and anti-Markovnikov insertion pathways occurs at similar rates. Moreover, a kinetic study comparing the rate for styrene and styrene-d_8 hydroarylation gave a KIE (Kinetic Isotopic Effect) of 1.06. This value suggests that no X-H cleavage occurs in the rate-limiting step,

therefore, C-H activation and migratory insertion steps might be discarded in favor of reductive elimination.[32]

Scheme 9. Deuterium Labeling Experiments

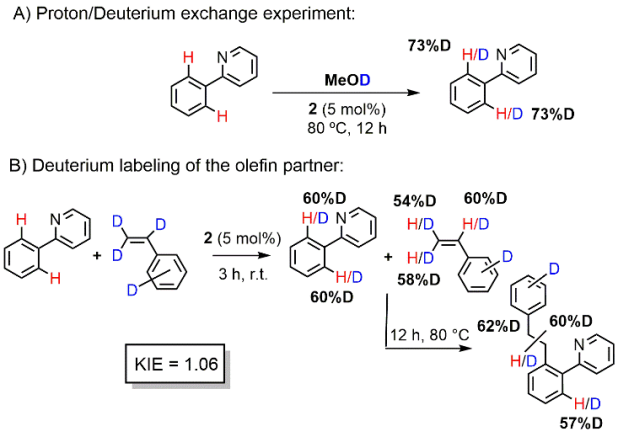

Based on the detected intermediates at low temperature and deuterium labeling experiments, a plausible mechanism for hydroarylation reactions is proposed in Scheme 10. The first step involves the coordination of the unsaturated substrate on the complex **2**. Subsequently, the insertion of the olefin/alkyne may occur either by hydrometallation into Rh-H bond or by carbometallation into Rh-C bond. However, a hydrometalation pathway is proposed in view of alkyl intermediates **7** and **8** detected in the reactivity studies. Furthermore, the insertion step via Markovnikov (route I) or anti-Markovnikov addition (route II) might yield the corresponding Rh-hydrocarbyl derivatives which would be in equilibrium, as confirmed by the deuterium-labeling experiments. Reductive elimination could be operative only for the linear anti-Markovnikov species to yield the C-C coupled organic product and a rhodium(I) species similar to detected intermediate **10**. Finally, C-H activation of 2-phenylpyridine within rhodium(I) species regenerates the catalytic active species.

Scheme 10. Proposed Catalytic Cycle for Hydroarylation

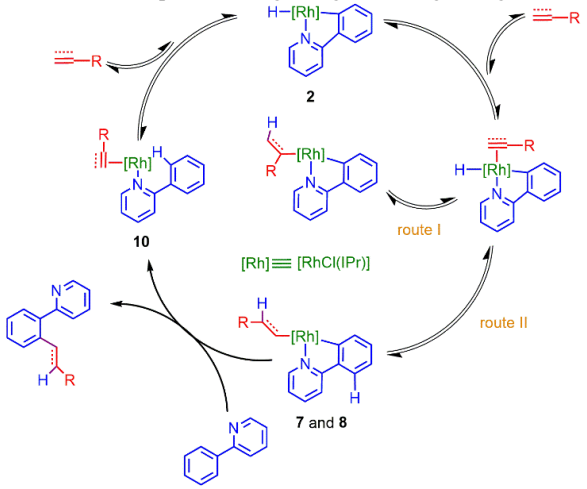

Theoretical Calculations on the Mechanism. A detailed DFT computational analysis on the mechanism of hydroarylation promoted by **2** has been carried out. All the energies (ΔG in kcal mol^{-1}) are relative to the starting point **A** and the corresponding reactants. Firstly, the hydroarylation of olefins was studied using propene as an alkene model (Figure 3). The structure of **A** consists of a square-planar rhodium(I) environment containing IPr, chlorido and 2-phenylpyridine ligands, the later displaying an agostic interaction between one *ortho*-phenyl C-H bond and the metallic center. This interaction is easily broken by coordination of propene to form **B**, similar to **10**, resulting in a net stabilization by 4.2 kcal mol^{-1}. Otherwise, compound **A** is a putative intermediate for the formation of the rhodium-hydride active species **D**, similar to **2**, via a low energy C-H activation process.[14d,16i,l] Next, anti-Markovnikov insertion of the olefin into the Rh-H bond takes place via **TSF** to give the Rh-alkyl complex **G,** similar to **8**. Finally, alkyl-aryl reductive elimination through **TSH** yields a rhodium square planar species **I**, similar to **A** but bearing a *ortho* alkyl-substituted 2-phenylpyridine, which lies 5.9 kcal mol^{-1} below **A**. Ligand exchange between 2-phenylpyridine and its functionalized counterpart closes this exergonic catalytic cycle. Among the three transition states, **TSH** has the highest energy, thus reductive elimination is rate-limiting, showing an overall barrier from **B** of 23.3 kcal mol^{-1}. Moreover, formation of **G** is a reversible process, in agreement with the experimental results and deuterium labeling experiments. Complex **8** was initially formed after treatment of **2** with styrene at low temperature, but evolves into the more stable η^2-olefin complex **10** at room temperature.

The unsuccessful double-alkylation of 2-phenylpyridine was also explained by DFT calculations. In a similar way as observed for **A**, coordination of a propene molecule to **I** to yield **J**, resulting in a stabilization of 8.9 kcal mol^{-1}, higher than that observed for **B**. From this point, the iteration of a similar pathway to that previously described via C-H activation (**TSK**), olefin insertion (**TSN**) and reductive elimination (**TSP**) results in the formation of **Q** bearing a doubly-alkylated 2-phenylpyridine ligand. The absolute energy levels of all these transition states are lower than those found for their counterparts **TSC**, **TSF**, and **TSH**, respectively. However, the higher energetic barrier from **J** to **TSP** in comparison with that from **B** to **TSH** (27.9 *vs* 23.3 kcal mol^{-1}), makes the second hydroarylation process unfeasible at the current temperature conditions. The reason for this fact is an additional stabilization of **J** with respect to **B**. Structural analysis of intermediate **J** reveals that two hydrogen atoms of the alkyl substituent of the 2-phenylpyridine lie at 3.130 and 3.424 Å to the negatively charged chlorine ligand, indicating that some type of weak electrostatic interaction might be present. Analysis of non-covalent interactions using the NCI method[33] reveals a weakly attractive interaction region which can be responsible of the additional stability of **J** compared to **B** (see SI).

The anti-Markovnikov selectivity of the alkene hydroarylation process has been also studied. Figure 4 shows the energy profile for the olefin insertion and reductive elimination steps for Markonikov (blue, left) and anti-Markovnikov additions (red, right). The first step displays similar energy barrier for the 2,1 or 1,2 insertion, 18.3 *vs* 17.9 kcal mol^{-1}, respectively. However, the transition state corresponding to the branched alkyl-phenyl reductive elimination (**TSH´**) is located 2.9 kcal mol^{-1} above **TSH**, therefore disfavoring the formation of the branched-alkyl functionalized phenylpyridine. Moreover, the uniform distribution of the deuterium atoms over the three olefinic positions of styrene observed in the H/D exchange experiments is explained by two facts: *i*) reductive elimination as rate-limiting step, and *ii*) similar energies observed for both insertion types (Scheme 9, B).

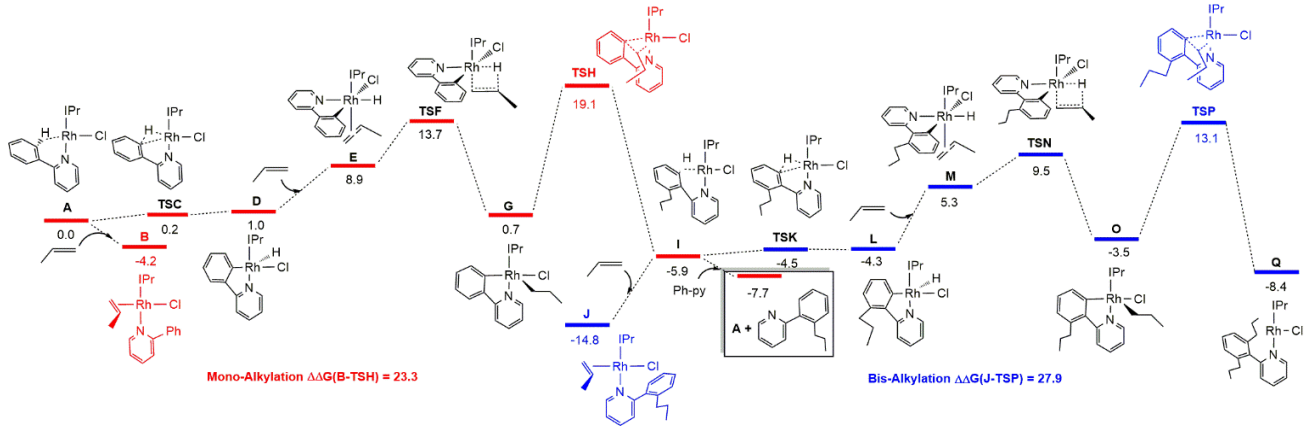

Figure 3. DFT calculations (ΔG in kcal mol^{-1}) along the energy surface for the hydroarylaton of olefins.

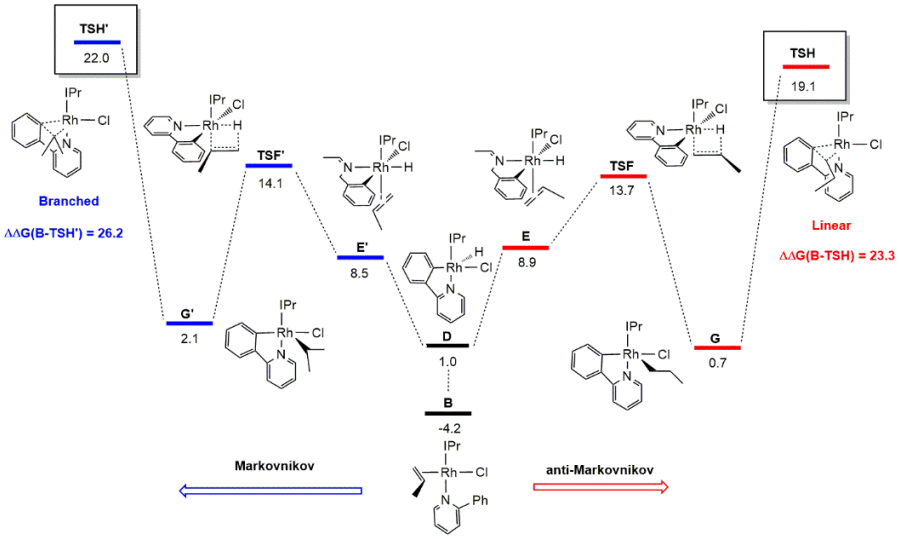

Figure 4. Computed energies (ΔG in kcal mol^{-1}) for the Markovnikov (blue) and anti-Markovnikov (red) olefin hydrometallation.

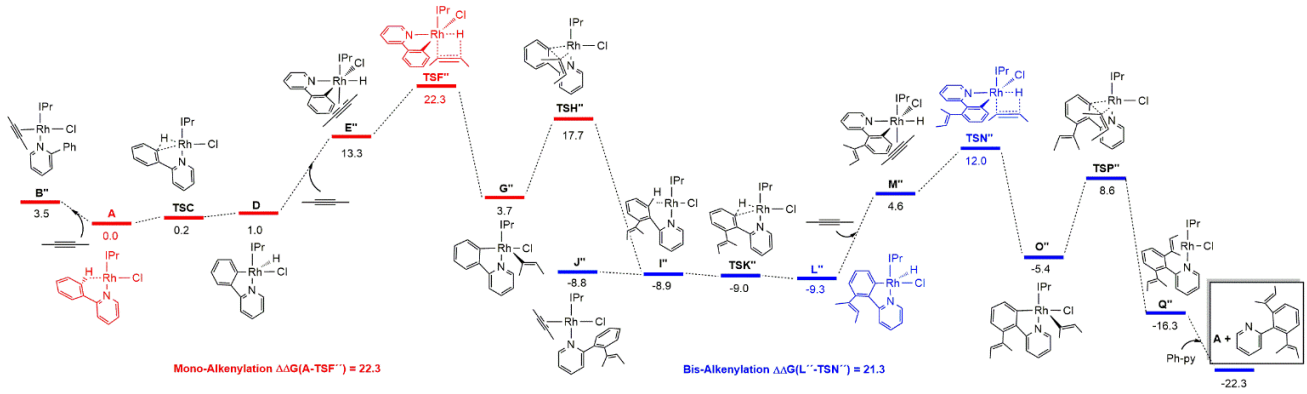

Figure 5. DFT calculations (ΔG in kcal mol^{-1}) for the hydroarylaton of alkynes.

Next, the alkyne hydroarylation processes were calculated (Figure 5). In this case, the coordination of a molecule of alkyne into **A** is disfavored by 3.5 kcal mol^{-1}. Another important difference is the rate-limiting step. In contrast to alkene hydroarylation, transition state for insertion step **TSF´´** is more disfavored than that of reductive elimination **TSH´´** (22.3 *vs* 17.7 kcal mol^{-1}). This is in agreement with the failure to detect experimentally any intermediate related to **G´´** after treatment of **2** with diphenylacetylene. The energetic barrier from **A** to **TSF´´** is lower than that observed for alkene hydroarylation (22.3 *vs* 23.3 kcal mol^{-1}). Moreover, according to the experimental results, the second alkyne hydroarylation with the alkenyl-functionalized phenylpyridine is faster than the first alkyne hydroarylation process. The energy barrier between the more stable rhodium-hydride intermediate **L''** and the higher energy transition state corresponding to the alkyne insertion, **TSN´´**, is only 21.3 kcal mol^{-1}. The origin of the different behavior of alkenes and alkynes seems to be

related to coordination of the unsaturated ligand to the corresponding square-planar agostic intermediates **A** or **I**. While coordination of alkene to **I** reduces the ground state energy of the intermediate **J** by 8.9 kcal mol^{-1}, the coordination of an alkyne to **I´´** is disfavored. The stabilization gained in the case of the alkenes increase the energetic barrier, thus hampering the catalytic process.

Finally, the relevant intermediate and transition state for determining the energetic barrier for the tandem alkylation/alkenylation process was calculated (Figure 6). A separation of 23.4 kcal mol^{-1} was found, which lies between that obtained for the operative double alkenylation and unfeasible double alkylation.

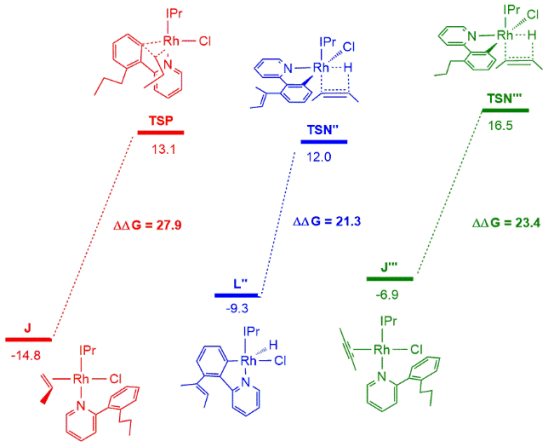

Figure 6. Comparison of energy barriers for double alkylation (left, red), double alkenylation (center, blue) and tandem alkylation/alkenylation (right, green).

CONCLUSION

A new NHC-rhodium-hydride complex RhClH{κ-N,κ-C-($C_{11}H_8N$)}(IPr) has been revealed as efficient catalyst for olefin isomerization and C-C coupling reactions. High selectivity for the formation of the *E*-regioisomer is observed in the isomerization of internal or terminal alkenes, including chain-walking processes, as a result of a favored β-elimination step. Hydroarylation of olefins with 2-phenylpyridine lead to the selective formation of linear mono-*ortho*-alkylated derivatives whereas internal alkynes afford bis-ortho-alkenylated compounds. The rhodium-hydride catalyst promotes tandem isomerization/hydroarylation processes and more interestingly alkylation/alkenylation reactions as a useful synthetic approach to functionalized styrenes.

Stoichiometric reactions at low temperature, deuterium labeling experiments, and DFT studies have revealed a mechanism entailing C-H activation, migratory insertion and reductive elimination. In the case of olefin hydroarylation, both C-H activation as well as migratory insertion are reversible, whereas reductive elimination is the rate-limiting step. However, migratory insertion is rate-limiting for alkyne hydroarylation. DFT calculations have disclosed a high barrier for the double alkylation process whereas tandem alkylation/alkenylation rate-determining step lies well below that and slightly above the operational double alkenylation. The origin for the different behavior of alkenes and alkynes arises from the coordination of the unsaturated substrates to a C-H agostic intermediate species. While coordination of alkynes is disfavored, alkenes stabilize agostic intermediates, therefore resulting in an increment of the barrier. An additional stabilization by non-covalent interactions between the mono-alkylated product and the chloride ligand renders the double alkylation process unfeasible.

EXPERIMENTAL SECTION

General Considerations. All reactions were carried out with rigorous exclusion of air using Schlenk-tube techniques. The reagents were purchased from commercial sources and were used as received. Organic solvents were dried by standard procedures and distilled under argon prior to use or obtained oxygen- and water-free from a Solvent Purification System (Innovative Technologies). The organometallic precursor [Rh(μ-Cl)(IPr)(η^2-coe)]$_2$ (**1**) was prepared as previously described in the literature.[18a] Chemical shifts (expressed in parts per million) are referenced to residual solvent peaks (^{1}H and ^{13}C{^{1}H}). Coupling constants, *J*, are given in Hz. Spectral assignments were achieved by combination of ^{1}H-^{1}H COSY, ^{13}C{^{1}H}-APT and ^{1}H-^{13}C HSQC/HMBC experiments. C, H, and N analyses were carried out in a Perkin-Elmer 2400 CHNS/O analyzer. High-resolution electrospray mass spectra (HRMS) were acquired using a MicroTOF-Q hybrid quadrupole time-of-flight spectrometer (Bruker Daltonics, Bremen, Germany). GC-MS analysis were recorder on an Agilent 5973 mass selective detector interfaced to an Agilent 6890 series gas chromatograph system, using a HP-5MS 5% phenyl methyl siloxane column (30 m x 250 mm with a 0.25 mm film thickness).

Preparation of RhClH{κ-N,κ-C-($C_{11}H_8N$)}(IPr) (2). A solution of dinuclear complex **1** (300 mg, 0.23 mmol) in 100 mL of toluene was treated with 2-phenylpyridine (67 μL, 0.470 mmoles) and stirred for 2h at 80°C. After filtration through Celite the solvent was evaporated to dryness. Addition of hexane induced the precipitation of a yellow solid, which was washed with hexane (3 x 4 mL) and dried in vacuo. Yield: 280 mg (87%). Anal. Calcd. for $C_{38}H_{45}N_3ClRh$: C, 66.91; H, 6.65; N, 6.16. found: C, 67.18; H, 6.77; N, 6.21.^{1}H NMR (500 MHz, toluene-d_8, 243 K): δ 9.64 (d, $J_{H\text{-}H}$ = 5.7, 1H, $H_{6\text{-}py}$), 7.2-6.8 (10H, H_{Ph}), 6.69 (d, $J_{H\text{-}H}$ = 8.0, 1H, $H_{3\text{-}py}$), 6.66 and 6.55 (both d, $J_{H\text{-}H}$ = 1.7, 2H, =CHN), 6.56 (dd, $J_{H\text{-}H}$ = 8.0, 7.4, 1H, $H_{4\text{-}py}$), 6.12 (dd, $J_{H\text{-}H}$ = 7.4, 5.7, 1H, $H_{5\text{-}py}$), 4.08, 3.79, 3.22, and 2.82 (all sept, $J_{H\text{-}H}$ = 7.4, 4H, C$\underline{H}$Me$_{IPr}$), 1.88, 1.65, 1.15, 1.06, 1.04, 1.02, 0.95, and 0.64 (all d, $J_{H\text{-}H}$ = 7.4, 24H, CH$\underline{Me}_{IPr}$), -24.67 (d, $J_{H\text{-}H}$ = 50.2, 1H, Rh-H). ^{13}C{^{1}H}-APT NMR (125.6 MHz, toluene-d_8, 243 K): δ 185.7 (d, $J_{C\text{-}Rh}$ = 57.0, Rh-C_{IPr}), 163.9 (d, $J_{C\text{-}Rh}$ = 32.0, Rh-C_{Ph}), 163.6 (d, $J_{C\text{-}Rh}$ = 2.0, $C_{2\text{-}py}$), 150.8 (s, $C_{6\text{-}py}$), 148.5, 147.7, 146.8, and 144.9 (all s, $C_{q\text{-}IPr}$), 146.9 (s, $C_{q\text{-}Ph}$), 139.9, 130.0, 129.8, 129.6, 128.4, 128.2, 124.2, 123.6, 123.5, and 123.2 (all s, CH_{Ph}), 139.3 and 135.4 (both s, C_qN), 136.2 (s, $C_{4\text{-}py}$), 121.7 and 121.3 (both s, =CHN), 120.7 (s, $C_{5\text{-}py}$), 116.5 (s, $C_{3\text{-}py}$), 29.4, 29.3, 28.6, and 28.3 (all s, C$\underline{H}$Me$_{IPr}$), 27.2, 26.3, 25.7, 25.6, 23.9, 23.6, 22.9, and 22.6 (all s, CH$\underline{Me}_{IPr}$).

In-situ Formation of RhCl(Et){κ-N,κ-C-($C_{11}H_8N$)}(IPr) (7). A NMR Young tube containing a toluene-d_8 solution of **2** (30 mg, 0.044 mmol) was charged with 2 bar of ethylene at 243 K. NMR Spectra were measured immediately at low temperature. ^{1}H NMR (400 MHz, toluene-d_8, 243 K): δ 10.07 (d, $J_{H\text{-}H}$ = 4.9, 1H, $H_{6\text{-}py}$), 7.2-6.4 (10H, H_{Ph}), 6.97 (d, $J_{H\text{-}H}$ = 7.4, 1H, $H_{3\text{-}py}$), 6.69 (dd, $J_{H\text{-}H}$ = 7.8, 7.4, 1H, $H_{4\text{-}py}$), 6.76 and 6.57 (both d, $J_{H\text{-}H}$ = 1.6, 2H, =CHN), 6.22 (dd, $J_{H\text{-}H}$ = 7.8, 4.9, 1H, $H_{5\text{-}py}$), 4.51, 3.58, 3.33, and 3.30 (all sept, $J_{H\text{-}H}$ = 7.4, 4H, C$\underline{H}$Me$_{IPr}$), 2.85 and 1.75 (both m, 2H, RhCH_2), 1.82, 1.77, 1.40, 1.33, 1.19, 1.12, 1.09, and 0.95 (all d, $J_{H\text{-}H}$ = 7.4, 24H, CH$\underline{Me}_{IPr}$), -0.10 (m, 3H, Rh-CH_2C$\underline{H}_3$). ^{13}C{^{1}H}-APT NMR (100.4 MHz, toluene-d_8, 243 K): δ 181.5 (d, $J_{C\text{-}Rh}$ = 60.8, Rh-

C_{IPr}), 172.9 (d, $J_{C\text{-}Rh}$ = 38.7, Rh-C_{Ph}), 163.8 (s, $C_{2\text{-}py}$), 150.9 (s, $C_{6\text{-}py}$), 149.1, 147.6, 145.4, and 144.2 (all s, $C_{q\text{-}IPr}$), 146.9 (s, $C_{q\text{-}Ph}$), 140.5, 130.4, 130.0, 129.8, 129.0, 127.0, 124.0, 123.9, 123.8, 123.3, 123.1, 121.6 (all s, CH_{Ph}, =CHN), 136.7 and 134.3 (both s, C_qN), 136.4 (s, $C_{4\text{-}py}$), 120.6 (s, $C_{5\text{-}py}$), 116.9 (s, $C_{3\text{-}py}$), 29.6, 29.4, 29.0, and 28.7 (all s, CH<u>Me</u>$_{IPr}$), 27.5, 26.9, 26.2, 26.1, 26.0, 23.8, 23.3, and 22.9 (all s, CH<u>Me</u>$_{IPr}$), 18.3 (d, $J_{C\text{-}Rh}$ = 32.4, Rh<u>C</u>H_2CH_3), 14.4 (s, $RhCH_2$<u>C</u>H_3).

In-situ Formation of RhCl(CH_2CH_2Ph){κ-N,κ-C-($C_{11}H_8N$)}(IPr) (IPr) (8). A solution of **2** (30 mg, 0.044 mmol) in toluene-d_8 (0.5 mL, NMR tube) at 243 K was treated with styrene (5 μL 0.044 mmol). The tube was kept at low temperature for 30 min before the recording of the spectra. ^{1}H NMR (400 MHz, toluene-d_8, 243 K): δ 10.18 (d, $J_{H\text{-}H}$ = 5.5, 1H, $H_{6\text{-}py}$), 7.4-6.9 (10H, H_{Ph}), 6.98 (d, $J_{H\text{-}H}$ = 8.2, 1H, $H_{3\text{-}py}$), 6.92 (dd, $J_{H\text{-}H}$ = 7.8, 7.1, 2H, $H_{m\text{-}Ph\text{-}st}$), 6.76 and 6.55 (both br, 2H, =CHN), 6.75 (dd, $J_{H\text{-}H}$ = 8.2, 6.7, 1H, $H_{4\text{-}py}$), 6.71 (t, $J_{H\text{-}H}$ = 7.1, 1H, $H_{p\text{-}Ph\text{-}st}$), 6.47 (d, $J_{H\text{-}H}$ = 7.8, 2H, $H_{o\text{-}Ph\text{-}st}$), 6.25 (dd, $J_{H\text{-}H}$ = 6.7, 5.5, 1H, $H_{5\text{-}py}$), 4.66, 3.47, 3.33, and 3.32 (all sept, $J_{H\text{-}H}$ = 6.3, 4H, C<u>H</u>Me$_{IPr}$), 2.94 and 1.74 (both m, 2H, RhC<u>H</u>$_2CH_2$), 2.17, and 1.68 (both m, 2H, $RhCH_2$C<u>H</u>$_2$), 1.94, 1.80, 1.27, 1.15, 1.14, 1.12, 0.96, and 0.59 (all d, $J_{H\text{-}H}$ = 6.3, 24H, CH<u>Me</u>$_{IPr}$). ^{13}C{^{1}H}-APT NMR (100.4 MHz, toluene-d_8, 243K): δ 181.2 (d, $J_{C\text{-}Rh}$ = 60.3, Rh-C_{IPr}), 172.4 (d, $J_{C\text{-}Rh}$ = 40.2, Rh-C_{Ph}), 164.0 (d, $J_{C\text{-}Rh}$ = 1.9, $C_{2\text{-}py}$), 151.0 (s, $C_{6\text{-}py}$), 149.1, 147.2, 145.3, 144.0 (all s, $C_{q\text{-}IPr}$), 146.9 (s, $C_{q\text{-}Ph}$), 142.1 (d, $J_{C\text{-}Rh}$ = 3.1, $C_{q\text{-}Ph\text{-}st}$), 140.6, 138.9, 130.0, 129.7, 125.2, 123.9, 123.8, 123.7, 123.1, and 121.6 (all s, CH_{Ph}), 136.7 (s, $C_{4\text{-}py}$), 136.4 and 134.4 (both s, C_qN), 128.1 (s, $C_{o\text{-}Ph\text{-}st}$), 127.5 (s, $C_{m\text{-}Ph\text{-}st}$), 125.4 and 124.6 (both s, =CHN), 123.3 ($C_{p\text{-}Ph\text{-}st}$), 120.7 (s, $C_{5\text{-}py}$), 117.0 (s, $C_{3\text{-}py}$), 40.2 (s, $RhCH_2$<u>C</u>H_2Ph), 29.7, 29.4, 28.9, and 28.7 (all s, <u>C</u>HMe$_{IPr}$), 23.4 (d, $J_{C\text{-}Rh}$ = 34.3, Rh<u>C</u>H_2CH_2Ph), 27.6, 27.0, 26.1, 26.0, 23.8, 23.4, 22.9, and 20.5 (all s, CH<u>Me</u>$_{IPr}$).

In-situ Formation of RhCl(η^2-CH_2=CHPh)(κ-N-2-phenylpyridine)(IPr) (10). A freshly prepared solution of **7** was warming to room temperature for 10 min and then cooled to low temperature for the recording of the spectra. ^{1}H NMR (400 MHz, toluene-d_8, 243K): δ 8.37 (d, $J_{H\text{-}H}$ = 5.7, 1H, $H_{6\text{-}py}$), 8.25 (d, $J_{H\text{-}H}$ = 7.6, 2H, $H_{o\text{-}PhPy}$), 7.60, 7.44, 7.22, and 7.12 (all d, $J_{H\text{-}H}$ = 8.0, 4H, $H_{m\text{-}IPr}$), 7.53 and 7.47 (both t, $J_{H\text{-}H}$ = 8.0, 2H, $H_{p\text{-}IPr}$), 7.31 (t, $J_{H\text{-}H}$ = 7.3, 1H, $H_{p\text{-}PhPy}$), 6.93 (dd, $J_{H\text{-}H}$ = 7.6, 7.3, 2H, $H_{m\text{-}PhPy}$), 6.80 (t, $J_{H\text{-}H}$ = 6.8, 1H, $H_{p\text{-}Ph\text{-}st}$), 6.56 and 6.09 (both br, 4H, $H_{Ph\text{-}st}$), 6.55 (m, 1H, $H_{4\text{-}py}$), 6.54 (m, 1H, $H_{3\text{-}py}$), 6.53 and 6.49 (both d, $J_{H\text{-}H}$ = 1.9, 2H, =CHN), 5.93 (dd, $J_{H\text{-}H}$ = 6.5, 5.7, 1H, $H_{5\text{-}py}$), 4.96, 4.30, 2.55, and, 2.11 (all sept, $J_{H\text{-}H}$ = 6.8, 4H, C<u>H</u>Me$_{IPr}$), 4.55 (dd, $J_{H\text{-}H}$ = 12.3, 7.6, 1H, C<u>H</u>=CH_2), 2.24 (d, $J_{H\text{-}H}$ = 7.6, 1H, CH=C<u>H</u>$_2$), 1.93, 1.74, 1.27, 1.20, 1.15, 1.13, 1.02, and 0.92 (all d, $J_{H\text{-}H}$ = 6.8, 24H, CH<u>Me</u>$_{IPr}$), 1.63 (d, $J_{H\text{-}H}$ = 12.3, 1H, CH=C<u>H</u>$_2$). ^{13}C{^{1}H}-APT NMR (100.4 MHz, toluene-d_8, 243K): δ 181.9 (d, $J_{C\text{-}Rh}$ = 54.0, Rh-C_{IPr}), 158.9 (s, $C_{2\text{-}py}$), 154.4 (s, $C_{6\text{-}py}$), 148.8, 148.6, 146.2, and 146.0 (all s, $C_{q\text{-}IPr}$), 146.3 (s, $C_{q\text{-}Ph\text{-}st}$) 140.6 (s, $C_{q\text{-}Ph}$), 138.1 and 137.9 (both s, C_qN), 134.4 (s, $C_{4\text{-}py}$), 129.8, 129.6, 125.2, 125.0, 123.8, 123.4 (all s, $C_{Ph\text{-}IPr}$), 128.5 (s, $C_{o\text{-}PhPy}$), 128.0, 127.7, and 123.2 (all s, $C_{Ph\text{-}st}$), 127.9 (s, $C_{m\text{-}PhPy}$), 127.6 (s, $C_{p\text{-}PhPy}$), 125.1 and 124.9 (both s, =CHN), 123.0 (s, $C_{3\text{-}py}$), 120.7 (s, $C_{5\text{-}py}$), 54.1 (d, $J_{C\text{-}Rh}$ = 16.1, <u>C</u>H=CH_2), 32.3 (d, $J_{C\text{-}Rh}$ = 15.6, CH=<u>C</u>H_2), 28.9, 28.7, 28.7, and 28.5 (all s, <u>C</u>HMe$_{IPr}$), 26.8, 26.7, 26.5, 26.2, 24.0, 23.7, 22.1, and 22.0 (all s, CH<u>Me</u>$_{IPr}$).

Standard conditions for hydroarylation of alkenes and alkynes with 2-phenylpyridine. A NMR tube containing a solution of 0.01 mmol of catalyst **2** in 0.5 mL of C_6D_6 was treated with 0.20 mmol of 2-phenylpyridine and 0.20 mmol of alkene or 0.40 mmol of alkyne and heated at 90 ºC. The reaction course was monitored by ^{1}H NMR and the conversion was determined by integration of the corresponding resonances of the alkyne and the products.

Standard conditions for tandem hydroarylation with 2-phenylpyridine. A NMR tube containing a solution of 0.01 mmol of catalyst **2** in 0.5 mL of C_6D_6 was treated with 0.20 mmol of 2-phenylpyridine and 0.20 mmol of alkene, which was heated at 90°C to obtain the monoalkylated compound. Afterwards, 0.20 mmol of alkyne was added to the NMR tube and heated at 90 ºC. The reaction course was monitored by ^{1}H NMR and the conversion was determined by integration of the corresponding resonances of the alkyne and the products.

Crystal Structure Determination. Single crystals of **2** for the X-ray diffraction studies were grown by diffusion of hexane into a toluene solution of **2**. X-ray diffraction data were collected at 100(2) K on a Bruker APEX SMART CCD diffractometer with graphite-monochromated Mo−Kα radiation (λ = 0.71073 Å) using 0.6° ω rotations. Intensities were integrated and corrected for absorption effects with SAINT–PLUS[34] and SADABS[35] programs, both included in APEX2 package. The structures were solved by the Patterson method with SHELXS-97[36] and refined by full matrix least-squares on F^2 with SHELXL-2014,[37] under WinGX.[38]

Crystal data for 2. $4(C_{38}H_{45}ClN_3Rh)\cdot C_7H_8$, M = 2820.64 g·mol^{-1}, monoclinic, $P2_1/n$, a = 22.2298(10) Å, b = 14.0027(6) Å, c = 23.0551(11) Å, β = 102.7880(10)°, V= 6998.5(5) Å^3, Z = 2, D_{calc} = 1.339 Mg·m^{-3}, μ = 0.596 mm^{-1}, F(000) = 2948, yellow prism, 0.283 x 0.260 x 0.090 mm^3, ϑ_{min} = 1.442°, ϑ_{max} = 28.702°, limiting indexes –29≤h≤29, -18≤k≤18, -30≤l≤30, reflections collected/unique 140709/17219 [R(int) = 0.0481], data/restraints/parameters 17219/17/851, GOF = 1.065, R_1 = 0.0335 [I>2σ (I)], wR^2 = 0.0752 (all data). Largest diff. peak/hole 0.853/–0.784 e·Å^{-3}.

Determination of rotational barriers. Full line-shape analysis of the dynamic ^{1}H NMR spectra of **5a** were carried out using the program gNMR (Cherwell Scientific Publishing Limited). The transverse relaxation time, T_2, was estimated at the lowest temperature. Activation parameters $\Delta H^{\neq}$ and $\Delta S^{\neq}$ were obtained by linear least-squares fit of the Eyring plot. Errors were computed by published methods.[39]

Computational details. All DFT theoretical calculations were carried out using the Gaussian program package.[40] The M06 method,[41] has been used for both energies and gradient calculations. All atoms were treated with the def2-SVP basis set[42] together with the corresponding core potential for Rh for geometry optimizations. Energies were further refined by single point calculations using the def2-TZVP basis set and solvent corrections using the SMD[43] approach for benzene as implemented in G09. The "ultrafine" grid was employed in all calculations. All reported energies are Gibbs free energies referred to a 1 M standard state using the correction proposed by Goddard III et al.[44] at 90º C including basis set and solvent corrections. The nature of the stationary points was confirmed by analytical frequency analysis, and transition states were characterized by a single imaginary frequency corresponding to the expected motion of the atoms. The NCIPLOT program[45] has been used for the NCI maps.

ASSOCIATED CONTENT

Supporting Information

The Supporting Information is available free of charge on the ACS Publications website at DOI: http://pubs.acs.org.

Miscellaneous information including NMR data of complexes and organic products (PDF).

Optimized coordinates for the computed compounds (XYZ).

Accession Codes

CCDC 1015896 contains the supplementary crystallographic data for this paper. These data can be obtained free of charge via www.ccdc.cam.ac.uk/data_request/cif, or by emailing da-ta_request@ccdc.cam.ac.uk, or by contacting The Cambridge Crys-tallographic Data Centre, 12 Union Road, Cambridge CB2 1EZ, UK; fax: +44 1223 336033.

AUTHOR INFORMATION

Corresponding Author

* E-mail:rcastar@unizar.es.

Notes

The authors declare no competing financial interest

ACKNOWLEDGMENT

Financial support from the Spanish Ministerio de Economía y Competitividad (MINECO/FEDER) under the Projects CTQ2013-42532-P and CTQ2016-75884-P, the CSIC under the Project Proyectos Intramurales Especiales (201680I011), and the Diputación General de Aragón (DGA/FSE-E42-17R) are gratefully acknowledged. A.D.G. thanks the Spanish Ministerio de Economía y Competitividad (MINECO) for the postdoctoral grant Juan de la Cierva - Incorporación 2015 (IJCI-2015-27029). Authors would like to acknowledge the use of Servicio General de Apoyo a la Investigación-SAI, Universidad de Zaragoza.

REFERENCES

(1) (a) Kakiuchi, F.; Murai, S. Catalytic C-H/Olefin Coupling. *Acc. Chem. Res.* **2002**, *35*, 826. (b) Godula, K.; Sames, D. C–H Bond Functionalization in Complex Organic Synthesis. *Science* **2006**, *312*, 67. (c) Park, Y. J.; Park, J.-W.; Jun, C.-H. Metal-Organic Cooperative Catalysis in C-H and C-C Bond Activation and Its Concurrent Recovery. *Acc. Chem. Res.* **2008**, *41*, 222. (d) Boutadla, Y.; Davies, D. L.; Macgregor, S. A.; Poblador-Bahamonde, A. I. Mechanisms of C–H Bond Activation: Rich Synergy Between Computation and Experiment. *Dalton Trans.* **2009**, 5820. (e) Colby, D. A.; Bergman, R. G.; Ellman, J. A. Rhodium-Catalyzed C-C Bond Formation via Heteroatom-Directed C-H Bond activation. *Chem. Rev.* **2010**, *110*, 624. (f) Rouquet, G.; Chatani, N. Catalytic Functionalization of $C(sp^2)$-H and $C(sp^3)$-H Bonds by Using Bidentate Directing Groups. *Angew. Chem. Int. Ed.* **2013**, *52*, 11726. (g) Gensch, T.; Hopkinson, M. N.; Glorius, F.; Wencel-Delord, J. Mild Metal-Catalyzed C–H Activation: Examples and Concepts. *Chem. Soc. Rev.* **2016**, *45*, 2900. (h) Dong, Z.; Ren, Z.; Thompson, S. J.; Xu, Y.; Dong, G. Transition-Metal-Catalyzed C−H Alkylation Using Alkenes. *Chem. Rev.* **2017**, *117*, 9333. (i) Chu, J. C. K.; Rovis, T. Complementary Strategies for Directed $C(sp^3)$-H Functionalization: A Comparison of Transition-Metal-Catalyzed Activation, Hydrogen Atom Transfer, and Carbene/Nitrene Transfer. *Angew. Chem. Int. Ed.* **2018**, *57*, 62.

(2) (a) Grimsdale, A. C.; Chan, K. L.; Martin, R. E.; Jokisz, P. G.; Holmes, A. B. Synthesis of Light-Emitting Conjugated Polymers for Applications in Electroluminescent Devices. *Chem. Rev.* **2009**, *109*, 897. (c) Wang, D.-H.; Yu, J.-Q. Highly Convergent Total Synthesis of (+)-Lithospermic Acid via a Late-Stage Intermolecular C-H Olefination. *J. Am. Chem. Soc.* **2011**, *133*, 5767. (d) Yamaguchi, J.; Yamaguchi, A. D.; Itami, K. C-H Bond Functionalization: Emerging Synthetic Tools for Natural Products and Pharmaceuticals. *Angew. Chem. Int. Ed.* **2012**, *51*, 8960.

(3) (a) Mirozoki, T.; Mori, K.; Ozaki, A. Arylation of Olefin With Aryl Iodide catalyzed by Palladium. *Bull. Chem. Soc. Jpn.* **1971**, *44*, 581. (b) Heck, R. F.; Nolley, J. P., Jr. Palladium-Catalyzed Vinylic Hydrogen Substitution Reactions with Aryl, Benzyl, and Styryl Halides *J. Org. Chem.* **1972**, *37*, 2320. (c) Johanson-Seechurn, C. C. C.; Kitching, M. O.; Colacot, T. J.; Snieckus, V. Palladium-Catalyzed Cross-Coupling: A Historical Contextual Perspective to the 2010 Nobel Prize *Angew. Chem. Int. Ed.* **2012**, *51*, 5062.

(4) (a) Fujiwara, Y.; Moritani, I.; Danno, S.; Asano, R.; Teranishi, S. Aromatic Substitution of Olefins. VI. Arylation of Olefins with Palladium(II) Acetate. *J. Am. Chem. Soc.* **1969**, *41*, 7166. (b) Jia, C.; Kitamura, T.; Fujiwara, Y. Catalytic Functionalization of Arenes and Alkanes via C-H Bond Activation. *Acc. Chem. Res.* **2001**, *34*, 633. (c) Le Bras, J.; Muzart, J. Intermolecular Dehydrogenative Heck Reactions. *Chem. Rev.* **2011**, *111*, 1170. (d) Ma, W.; Gandepaan, P.; Li, J.; Ackermann, L. Recent Advances in Positional-Selective Alkenylations: Removable Guidance for Twofold C–H Activation. *Org. Chem. Front.* **2017**, *4*, 1435.

(5) (a) Zhang, Y.-H; Shi, B.-F.; Yu, J.-Q. Pd(II)-Catalyzed Olefination of Electron-Deficient Arenes Using 2,6-Dialkylpyridine Ligands *J. Am. Chem. Soc.* **2009**, *131*, 5072. (b) Patureau, F. W.; Besset, T.; Glorius, F. Rhodium-Catalyzed Oxidative Olefination of C–H Bonds in Acetophenones and Benzamides. *Angew. Chem. Int. Ed.* **2011**, *50*, 1064. (c) She, Z.; Shi, Y.; Huang, Y.; Cheng, Y.; Song, F.; You, J. Versatile Palladium-Catalyzed C–H Olefination of (Hetero)Arenes at Room Temperature. *Chem. Commun.* **2014**, *50*, 13914. (d) Li, S.; Ji, H.; Cai, L.; Li, G. Pd(II)-Catalyzed Remote Regiodivergent *ortho*- and *meta*-C–H Functionalizations of Phenylethylamines. *Chem. Sci.* **2015**, *6*, 5595. (e) Bu, Q.; Rogge, T.; Kotek, V.; Ackermann, L. Distal Weak Coordination of Acetamides in Ruthenium(II)-Catalyzed C-H Activation Processes. *Angew. Chem. Int. Ed.* **2018**, *57*, 765.

(6) (a) Nevado, C.; Echavarren, A. Transition Metal-Catalyzed Hydroarylation of Alkynes. *Synthesis* **2005**, 167. (b) Wang, X.; Zhou, L.; Lu, W. Hydroarylation of Alkynes via Aryl C–H Bond Cleavage *Curr. Org. Chem.* **2010**, *14*, 289. (c) Boyarskiy, V. P.; Ryabukhin, D. S.; Bokach, N. A.; Vasilyev, A. V. Alkenylation of Arenes and Heteroarenes with Alkynes. *Chem. Rev.* **2016**, *116*, 5894.

(7) (a) Jia, C.; Piao, D.; Oyamada, J.; Lu, W.; Fujiwara, Y. Efficient Activation of Aromatic C-H Bonds for Addition to C-C Multiple Bonds. *Science* **2000**, *287*, 1992. (b) Reetz, M.; Sommer, K. Gold-Catalyzed Hydroarylation of Alkynes. *Eur. J. Org. Chem.* **2003**, 3485. (c) Biffis, A.; Tubaro, C.; Baron, M. Advances in Transition-Metal-Catalysed Alkyne Hydroarylations. *Chem. Rec.* **2016**, *16*, 1742.

(8) (a) Boese, W. T.; Goldman, A. S. Insert ion of Acetylenes into Carbon-Hydrogen Bonds Catalyzed by Rhodium-Trimethylphosphine Complexes. *Organometallics* **1991**, *10*, 782. (b) Nakao, Y.; Kashihara, N.; Kanyiva, S.; Hiyama, T. Nickel-Catalyzed Alkenylation and Alkylation of Fluoroarenes via Activation of C-H Bond over C-F Bond. *J. Am. Chem. Soc.* **2008**, *130*, 16170. (c) Mukai, T.; Hirano, K.; Satoh, T.; Miura, M. Nickel-Catalyzed C-H Alkenylation and Alkylation of 1,3,4-Oxadiazoles with Alkynes and Styrenes. *J. Org. Chem.* **2009**, *74*, 6410. (d) Schipper, D. J.; Hutchinson, M.; Fagnou, K. Rhodium(III)-Catalyzed Intermolecular Hydroarylation of Alkynes. *J. Am. Chem. Soc.* **2010**, *132*, 6910. (e) Guihaumé, J.; Halbert, S.; Eisenstein, O.; Perutz, R. N. Hydrofluoroarylation of Alkynes with Ni Catalysts. C−H Activation via Ligand-to-Ligand Hydrogen Transfer, an Alternative to Oxidative Addition. *Organometallics* **2012**, *31*, 1300.

(9) (a) Murai, S.; Kakiuchi, F.; Sekine, S.; Tanaka, Y.; Katami, A.; Sonoda, M.; Chatani, N. Efficient Catalytic Addition of Aromatic Carbon-Hydrogen Bonds to Olefins. *Nature* **1993**, *366*, 529. (b) Kakiuchi, F.; Yamamoto, Y. Chatani, N. Murai, S. Catalytic Addition of Aromatic C-H Bonds to Acetylenes. *Chem. Lett.* **1995**, 681. (c) Trost, B. M.; Imi, K.; Davies, I. W. Elaboration of Conjugated Alkenes Initiated by Insertion into a Vinylic C-H Bond. *J. Am. Chem. Soc.* **1995**, *117*, 5371. (d) Kakiuchi, F.; Kochi, T.; Murai, S. Chelation-Assisted Regioselective Catalytic Functionalization of C–H, C–O, C–N and C–F Bonds. *Synlett.* **2014**, *25*, 2390. (e) Manikandan, R.; Jeganmohan, M. Recent Advances in the Ruthenium-Catalyzed Hydroarylation of Alkynes with Aromatics: Synthesis of Trisubstituted Alkenes. *Org. Biomol. Chem.* **2015**, *13*, 10420.

(10) (a) Grellier, M.; Vendier, L.; Chaudret, B.; Albinati, A.; Rizzato, S.; Mason, S.; Sabo-Etienne, S. Synthesis, Neutron Structure, and Reactivity of the Bis(dihydrogen) Complex $RuH_2(\eta^2\text{-}H_2)_2(PCyp_3)_2$ Stabilized by Two Tricyclopentylphosphines. *J. Am.*

Chem. Soc. **2005**, *127*, 17592. (b) Cheng, K.; Yao, B.; Zhao, J.; Zhang, Y. $RuCl_3$-Catalyzed Alkenylation of Aromatic C-H Bonds with Terminal Alkynes. *J. Org. Lett.* **2008**, *10*, 5309. (c) Martinez, R.; Simon, M.-O.; Chevalier, R.; Pautigny, C.; Gente, J.-P.; Darses, S. C-C Bond Formation via C-H Bond Activation Using an in Situ-Generated Ruthenium Catalyst. *J. Am. Chem. Soc*. **2009**, *131*, 7887. (d) Hashimoto, Y.; Hirano, K.; Satoh, T.; Kakiuchi, F.; Miura, M. Ruthenium(II)-Catalyzed Regio- and Stereoselective Hydroarylation of Alkynes via Directed C-H Functionalization. *Org. Lett*. **2012**, *14*, 2058. (e) Zhao, P.; Niu, R.; Wang, F.; Han, K.; Li, X. Rhodium(III)- and Ruthenium(II)-Catalyzed Olefination of Isoquinolones. *Org. Lett.* **2012**, *14*, 4166. (f) Itoh, M.; Hashimoto, Y.; Hirano, K.; Satoh, T.; Miura, M. Ruthenium-Catalyzed ortho-Alkenylation of Phenylphosphine Oxides through Regio- and Stereoselective Alkyne Insertion into C−H Bonds. *J. Org. Chem.* **2013**, *78*, 8098. (g) Padala, K.; Jeganmohan, M. Ruthenium-Catalyzed Highly Regio- and Stereoselective Hydroarylation of Aromatic Sulfoxides with Alkynes via C–H Bond Activation. *Chem. Commun.* **2014**, *50*, 14573. (h) Li, X. G.; Liu, K.; Zou, G.; Liu, P. N. Ruthenium-Catalyzed Alkenylation of Arenes with Alkynes or Alkenes by 1,2,3-Triazole-Directed C–H Activation. *Eur. J. Org. Chem.* **2014**, 7878. (i) Manikandan, R.; Jeganmohan, M. Ruthenium-Catalyzed Hydroarylation of Anilides with Alkynes: An Efficient Route to Ortho-Alkenylated Anilines. *Org. Lett.* **2014**, *16*, 912. (j) Villuendas, P.; Urriolabeitia, E. P. Ru-Catalyzed Regioselective CH-Hydroarylation of Alkynes with Benzylthioethers Using Sulfur as Directing Group. *Org. Lett*. **2015**, *17*, 3178. (k) Hu, F.; Szostak, M. Ruthenium(0)-Catalyzed Hydroarylation of Alkynes Via Ketone-Directed C–H Functionalization Using In Situ-Generated Ruthenium Complexes. *Chem. Commun.* **2016**, *52*, 9715. (l) Cheng, H.; Hernández, J. G.; Bolm, C. Mechanochemical Ruthenium-Catalyzed Hydroarylations of Alkynes under Ball-Milling Conditions. *Org. Lett*. **2017**, *19*, 6284.

(11) (a) Satoh, T.; Nishinaka, Y.; Miura, M.; Nomura, M. Iridium-Catalyzed Regioselective Reaction of 1-Naphthols with Alkynes at the *peri*-Position. *Chem. Lett.* **1999**, 615. (b) Tsuchikama, K.; Kasagawa, M.; Hashimoto, Y.-K.; Endo, K.; Shibata, T. Cationic Iridium–BINAP Complex-Catalyzed Addition of Aryl Ketones to Alkynes and Alkenes via Directed C–H Bond Cleavage. *J. Organomet. Chem*. **2008**, *693*, 3939. (c) Nagamoto, M.; Fukada, J.-i.; Hatano, M.; Yorimitsu, H.; Nishimura, T. Hydroxoiridium-Catalyzed Hydroarylation of Alkynes and Bicycloalkenes with N□Sulfonylbenzamides. *Org. Lett*. **2017**, *19*, 5952.

(12) (a) Gao, K.; Lee, P.-S.; Fujita, T.; Yoshikai, N. Cobalt-Catalyzed Hydroarylation of Alkynes through Chelation-Assisted C-H Bond Activation. *J. Am. Chem. Soc*. **2010**, *132*, 12249. (b) Lee, P.-S.; Fujita, T.; Yoshikai, N. Cobalt-Catalyzed, Room-Temperature Addition of Aromatic Imines to Alkynes via Directed C-H Bond Activation. *J. Am. Chem. Soc*. **2011**, *133*, 17283. (c) Fallon, B. J.; Derat, E.; Amatore, M.; Aubert, C.; Chemla, F.; Ferreira, F.; Perez-Luna, A.; Petit, M. C−H Activation/Functionalization Catalyzed by Simple, Well-Defined Low-Valent Cobalt Complexes. *J. Am. Chem. Soc*. **2015**, *137*, 2448. (d) Wang, S.; Hou, J.-T.; Feng, M.-L.; Zhang, X.-Z.; Chen, S.-Y.; Yu, X.-Q. Cobalt(III)-Catalyzed Alkenylation of Arenes and 6-Arylpurines with Terminal Alkynes: Efficient Access to Functional Dyes. *Chem. Commun.* **2016**, *52*, 2709. (e) Bera, S. S.; Debbarma, S.; Ghosh, A. K.; Chand, S.; Maji, M. S. Cp^*Co^{III}−Catalyzed syn-Selective C−H Hydroarylation of Alkynes Using Benzamides: An Approach Toward Highly Conjugated Organic Frameworks. *J. Org. Chem.* **2017**, *82*, 420. (f) Sen, M.; Rajesh, N.; Emayavaramban, B.; Premkumar, J. R.; Sundararaju, B. Isolation of Cp^*Co^{III}–Alkenyl Intermediate in Efficient Cobalt-Catalyzed C-H Alkenylation with Alkynes. *Chem. Eur. J.* **2018**, *24*, 342.

(13) Zhou, B.; Chen, H.; Wang, C. Mn-Catalyzed Aromatic C−H Alkenylation with Terminal Alkynes. *J. Am. Chem. Soc*. **2013**, *135*, 1264.

(14) (a) Lim, Y.-G.; Lee, K-H.; Koo, B. T.; Kang, J.-B. Rhodium(I)-Catalyzed *ortho*-Alkenylation of 2-Phenylpyridine with Alkynes. *Tet. Lett.* **2001**, *42*, 7609. (b) Lim, S.-G.; Lee. J. H.; Moon, C. W.; Hong, J.-B.; Jun, C.-H. Rh(I)-Catalyzed Direct *ortho*-Alkenylation of Aromatic Ketimines with Alkynes and Its Application to the Synthesis of Isoquinoline Derivatives. *Org. Lett.* **2003**, *5*, 2759. (c) Tsuchikama, K.; Kuwata, Y.; Tahara, Y.-k.; Yoshinami, Y.; Shibata, T. Rh-Catalyzed Cyclization of Diynes and Enynes Initiated by Carbonyl-Directed Activation of Aromatic and Vinylic C-H Bonds. *Org. Lett.* **2007**, *9*, 3097. (d) Kwak, J.; Ohk, Y.; Jung, Y.; Chang, S. Rollover Cyclometalation Pathway in Rhodium Catalysis: Dramatic NHC Effects in the C−H Bond Functionalization. *J. Am. Chem. Soc*. **2012**, *134*, 17778. (e) Zhou, W.; Yang, Y.; Wang, Z.; Deng, G.-J. Rhodium-Catalyzed Intermolecular Hydroarylation of Internal Alkynes with N-1-Phenylbenzotriazoles. *Org. Biomol. Chem.* **2014**, *12*, 251. (f) Martínez, A. M.; Echavarren, J.; Alonso, I.; Rodríguez, N.; Gómez Arrayás, R.; Carretero, J. C. Rh^{I}/Rh^{III} catalyst-controlled divergent aryl/heteroaryl C–H bond functionalization of picolinamides with alkynes. *Chem. Sci*. **2015**, *6*, 5802. (g) Mo, F.; Lim; H. N.; Dong, G. Bifunctional Ligand-Assisted Catalytic Ketone α□Alkenylation with Internal Alkynes: Controlled Synthesis of Enones and Mechanistic Studies. *J. Am. Chem. Soc*. **2015**, *137*, 15518. (h) Chen, B.; Jiang, Y.; Cheng, J.; Yu, J.-T. Rhodium-Catalyzed Hydroarylation of Alkynes via Tetrazole-Directed C–H Activation. *Org. Biomol. Chem*. **2015**, *13*, 2901. (i) Shibata, K.; Natsui, S.; Chatani, N. Rhodium-Catalyzed Alkenylation of C−H Bonds in Aromatic Amides with Alkynes. *Org. Lett.* **2017**, *19*, 2234. (j) Kathiravan, S.; Nicholls, I. A. Rhodium(III)-Catalysed, Redox-Neutral $C(sp^2)$-H Alkenylation Using Pivalimide as a Directing Group with Internal Alkynes. *Tetrahedron Lett.* **2017**, *58*, 1.

(15) (a) Hermann, W. N-Heterocyclic Carbenes: A NewConcept in Organometallic Catalysis. *Angew. Chem. Int. Ed*. **2002**, *41*, 1290. (b) Díez-González, S.; Marion, N.; Nolan, S. P. N-Heterocyclic Carbenes in Late Transition Metal Catalysis. *Chem. Rev*. **2009**, *109*, 3612. (c) Hahn, F. E. Substrate Recognition and Regioselective Catalysis with Complexes Bearing NR,NH-NHC Ligands. *ChemCatChem* **2013**, *5*, 419. (d) Hopkinson, M. N.; Richter, C.; Schedler M.; F. Glorius, F. An Overview of N-heterocyclic Carbenes. *Nature,* **2014**, *510*, 485. (e) Froese, R. D. J.; Lombardi, C.; Pompeo, M.; Rucker, R. P. Organ, M. G. Designing Pd−N-Heterocyclic Carbene Complexes for High Reactivity and Selectivity for Cross-Coupling Applications. *Acc. Chem. Res*. **2017**, *50*, 2244. (f) Peris, E. Smart N□Heterocyclic Carbene Ligands in Catalysis. *Chem. Rev.* **2008**, *118*, 9988.

(16) (a) Muehlhofer, M.; Strassner, T.; Herrrmann, W. A. New Catalyst Systems for the Catalytic Conversion of Methane into Methanol. *Angew. Chem. Int. Ed.* **2002**, *41*, 1745. (b) Fructos, M. R.; Belderrain, T. R.; de Frémont P.; Scott, N. M.; Nolan, S. P.; Díaz-Requejo, M. M.; Pérez, P. J. A Gold Catalyst for Carbene-Transfer Reactions from Ethyl Diazoacetate. *Angew. Chem. Int. Ed*. **2005**, *44*, 5284. (c) Corberán, R.; Sanau, M.; Peris, E. Highly Stable Cp*-Ir(III) Complexes with N-Heterocyclic Carbene Ligands as C-H Activation Catalysts for the Deuteration of Organic Molecules. *J. Am. Chem. Soc*. **2006**, *128*, 3974. (d) Lewis, J. C.; Bergman, R. G.; Ellman, J. A. Direct Functionalization of Nitrogen Heterocycles via Rh-Catalyzed C-H Bond Activation. *Acc. Chem. Res*. **2008**, *41*, 1013. (e) Kim, M.; Kwak, J.; Chang, S. Rhodium/N-Heterocyclic Carbene Catalyzed Direct Intermolecular Arylation of sp^2 and sp^3 C-H Bonds with Chelation Assistance. *Angew. Chem. Int. Ed.* **2009**, *48*, 8935. (f) Oonishi, Y.; Kitano, Y.; Sato, Y. Csp^3-H Bond Activation Triggered by Formation of Metallacycles: Rhodium(I)-Catalyzed Cyclopropanation/Cyclization of Allenynes. *Angew. Chem. Int. Ed.* **2012**, *51*, 7305. (g) Zhang, J.; Ugrinov, A.; Zhao, P. Ruthenium(II)/N-Heterocyclic Carbene Catalyzed [3+2] Carbocyclization with Aromatic N_H Ketimines and Internal Alkynes. *Angew. Chem. Int. Ed.* **2013**, *52*, 6681. (h) Mo, F.; Dong, G. Regioselective Ketone *a*-Alkylation with Simple Olefins via Dual Activation. *Science* **2014**, *345*, 68. (i) Dang, Y.; Qu, S.; Tao, Y.; Deng, X.; Wang, Z.-X. Mechanistic Insight into Ketone α□Alkylation with Unactivated Olefins via C−H Activation Promoted by Metal−Organic Cooperative Catalysis (MOCC): Enriching the MOCC Chemistry. *J. Am. Chem. Soc*. **2015**, *137*, 6279. (j) Nett, A. J.; Zhao, W.; Zimmerman, P. M.; Montgomery, J. Highly Active Nickel Catalysts for C−H Functionalization Identified through Analysis of Off-Cycle Intermediates. *J. Am. Chem. Soc*. **2015**, *137*, 7636. (k) Henrion, M.; Ritleng, V.; Chetcuti, M. J. Nickel N□Heterocyclic Carbene-Catalyzed C−C Bond Formation: Reactions and Mechanistic Aspects. *ACS Catal*. **2015**, *5*, 1283. (l) Rubio-Pérez, L.; Iglesias, M.; Munárriz, J.; Polo, V.; Passarelli, V.; Pérez-Torrente, J. J.; Oro, L. A. A Well-Defined NHC–Ir(III) Catalyst for the Silylation of Aromatic C–H Bonds: Substrate Survey and Mechanistic

Insights. *Chem. Sci.* **2017**, *8*, 4811. (m) Xu, W.; Yoshikai, N. Pivalophenone Imine as a Benzonitrile Surrogate for Directed C–H Bond Functionalization. *Chem. Sci.* **2017**, *8*, 5299.

(17) (a) Di Giuseppe, A.; Castarlenas, R.; Pérez-Torrente, J. J.; Lahoz, F. J.; Polo, V.; Oro, L. A. Mild and Selective H/D Exchange at the β Position of Aromatic α-Olefins by N-Heterocyclic Carbene–Hydride–Rhodium Catalysts *Angew. Chem. Int. Ed.* **2011**, *50*, 3938. (b) Azpíroz, R.; Di Giuseppe, A.; Castarlenas, R.; Pérez-Torrente, J. J.; Oro, L. A. A New Access to 4H-Quinolizines from 2-Vinylpyridine and Alkynes Promoted by Rhodium–N-Heterocyclic-Carbene Catalysts. *Chem. Eur. J.* **2013**, *19*, 3812. (c) Rubio-Pérez, L.; Azpíroz, R.; Di Giuseppe, A.; Polo, V.; Castarlenas, R.; Pérez-Torrente, J. J.; Oro, L. A. Pyridine-Enhanced Head-to-Tail Dimerization of Terminal Alkynes by a Rhodium–N-Heterocyclic-Carbene Catalyst *Chem. Eur. J.* **2013**, *19*, 15304. (d) Azpíroz, R.; Rubio-Pérez, L.; Castarlenas, R.; Pérez-Torrente, J. J.; Oro, L. A. gem-Selective Cross-Dimerization and Cross-Trimerization of Alkynes with Silylacetylenes Promoted by a Rhodium–Pyridine–N-Heterocyclic Carbene Catalyst. *ChemCatChem* **2014**, *6*, 2587. (e) Di Giuseppe, A.; Castarlenas, R.; Pérez-Torrente, J. J.; Lahoz, F. J.; Oro, L. A. Hydride-Rhodium(III)-N-Heterocyclic Carbene Catalysts for Vinyl-Selective H/D Exchange: A Structure–Activity Study *Chem. Eur. J.* **2014**, *20*, 8391. (f) Azpíroz, R.; Rubio-Pérez, L.; Di Giuseppe, A.; Passarelli, V.; Lahoz, F. J.; Castarlenas, R.; Pérez-Torrente, J. J.; Oro, L. A. Rhodium(I)-N-Heterocyclic Carbene Catalyst for Selective Coupling of N□Vinylpyrazoles with Alkynes via C−H Activation. *ACS Catal* **2014**, *4*, 4244. (g) Rubio-Pérez, L.; Iglesias, M.; Castarlenas, R.; Polo, V.; Pérez-Torrente, J. J.; Oro, L. A. Selective C-H Bond Functionalization of 2-(2-Thienyl)-pyridine by a Rhodium N-Heterocyclic Carbene Catalyst. *ChemCatChem* **2014**, *6*, 3192. (h) Azpíroz, R.; Di Giuseppe, A.; Passarelli, V.; Pérez-Torrente, J. J.; Oro, L. A.; Castarlenas, R. Rhodium−N-Heterocyclic Carbene Catalyzed Hydroalkenylation Reactions with 2-Vinylpyridine and 2-Vinylpyrazine: Preparation of Nitrogen-Bridgehead Heterocycles. *Organometallics*, **2018**, *37*, 1695.

(18) (a) Yu, X.-Y.; Patrick, B. O.; James, B. R. Rhodium(III) Peroxo Complexes Containing Carbene and Phosphine Ligands. *Organometallic*s **2006**, *25*, 4870. (b) Di Giuseppe, A.; Castarlenas, R.; Pérez-Torrente, J. J.; Crucianelli, M.; Polo, V.; Sancho, R.; Lahoz, F. J.; Oro, L. A. Ligand-Controlled Regioselectivity in the Hydrothiolation of Alkynes by Rhodium N-Heterocyclic Carbene Catalysts. *J. Am. Chem. Soc.* **2012**, *134*, 8171. (c) Zenkina, O. V.; Keske, E. C.; Kochhar, G. S.; Wang, R.; Crudden, C. M. Heteroleptic Rhodium NHC Complexes with Pyridine-Derived Ligands: Synthetic Accessibility and Reactivity Towards Oxygen. *Dalton Trans.* **2013**, *42*, 2282.

(19) (a) Lee, D.-H.; Kwon, K.-H.; Yi, C. S. Selective Catalytic C–H Alkylation of Alkenes with Alcohols. *Science* **2011**, *333*, 1613. (b) Kim, J.; Pannilawithana, N.; Yi, C. S. Catalytic Tandem and One-Pot Dehydrogenation–Alkylation and −Insertion Reactions of Saturated Hydrocarbons with Alcohols and Alkenes. *ACS Catal.* **2016**, *6*, 8395.

(20) (a) Li, W.; Arockiam, P. B.; Fischmeister, C.; Bruneau, C.; Dixneuf, P. H. C–H Bond Functionalisation with $[RuH(codyl)_2]BF_4$ Catalyst Precursor. *Green Chem.* **2011**, *13*, 2315. (b) Larsen, M. A.; Cho, S. H.; Hartwig, J. Iridium-Catalyzed, Hydrosilyl-Directed Borylation of Unactivated Alkyl C−H Bonds. *J. Am. Chem. Soc.* **2016**, *138*, 762.

(21) (a) Cramer, R. Olefin Coordination Compounds of Rhodium: The Barrier to Rotation of Coordinated Ethylene and the Mechanism of Olefin Exchange. *J. Am. Chem. Soc.* **1964**, *86*, 217. (b) Gauthier, D.; Lindhardt, A. T.; Olsen, E. P. K. Overgaard, J.; Skrydstrup, T. In Situ Generated Bulky Palladium Hydride Complexes as Catalysts for the Efficient Isomerization of Olefins. Selective Transformation of Terminal Alkenes to 2-Alkenes. *J. Am. Chem. Soc.* **2010**, *132*, 7998. (c) Scarso, A.; Colladon, M.; Sgarbossa, P.; Santo, C.; Michelin, R. A.; Strukul, G. Highly Active and Selective Platinum(II)-Catalyzed Isomerization of Allylbenzenes: Efficient Access to (E)-Anethole and Other Fragrances via Unusual Agostic Intermediates. *Organometallics* **2010**, *29*, 1487. (d) Knapp, S. M. M.; Shaner, S. E.; Kim, D.; Shopov, D. Y.; Tendler, J. A.; Pudalov, D. M.; Chianese, A. R. Mechanistic Studies of Alkene Isomerization Catalyzed by CCC Pincer Complexes of Iridium. *Organometallics* **2014**, *33*, 473. (e) Larsen, C. R.; Erdogan, G.; Grotjahn, D. B. General Catalyst Control of the Monoisomerization of 1□Alkenes to trans-2-Alkenes. *J. Am. Chem. Soc.* **2014**, *136*, 1226. (f) Kita, M. R.; Miller, A. J. M. An Ion-Responsive Pincer-Crown Ether Catalyst System for Rapid and Switchable Olefin Isomerization. *Angew. Chem. Int. Ed.* **2017**, *56*, 5498.

(22) (a) Jun, C.-H.; Lee, H.; Park, J.-B.; Lee, D.-Y. Catalytic Activation of C-H and C-C Bonds of Allylamines via Olefin Isomerization by Transition Metal Complexes. *Org. Lett.* **1999**, *1*, 2161. (b) Seayad, A.; Ahmed, M.; Klein, H.; Jackstell, R.; Gross, T.; Beller, M. Internal Olefins to Linear Amines. *Science* **2002**, *297*, 1676. (c) Dobereiner, G. E.; Erdogan, G.; Larsen, C. R.; Grotjahn, D. B., Schrock, R. R. A One-Pot Tandem Olefin Isomerization/Metathesis-Coupling (ISOMET) Reaction. *ACS Catal* **2014**, *4*, 3069. (d) Bair, J. S.; Schramm, Y.; Sergeev, A. G.; Clot, E.; Eisenstein, O.; Hartwig, J. F. Linear-Selective Hydroarylation of Unactivated Terminal and Internal Olefins with Trifluoromethyl-Substituted Arenes. *J. Am. Chem. Soc.* **2014**, *136*, 13098. (e) Hamasaki, T.; Aoyama, Y.; Kawasaki, J.; Kakiuchi, F.; Kochi, T. Chain Walking as a Strategy for Carbon−Carbon Bond Formation at Unreactive Sites in Organic Synthesis: Catalytic Cycloisomerization of Various 1,n□Dienes. *J. Am. Chem. Soc.* **2015**, *137*, 16163. (f) Sommer, H.; Juliá-Hernández, Martin, R.; Marek, I. Walking Metals for Remote Functionalization. *ACS Cent. Sci.* **2018**, *4*, 153. (g) Zhou, F.; Zhu, J.; Zhang, Y.; Zhu, S. NiH-Catalyzed Reductive Relay Hydroalkylation: A Strategy for the Remote C(sp3)-H Alkylation of Alkenes. *Angew. Chem. Int. Ed.* **2018**, *130*, 4122.

(23) (a) Yen, S. K.; Young, D. J.; Huynh, H. V.; Koh, L. L.; Hor, T. S. A. Unexpected Coordination Difference in Geometric-Isomerism Between N,S- and N,N-Heterocyclic Carbenes in Cyclometallated Platinum(II). *Chem. Commun*. **2009**, 6831. (b) Kim, Y.-Y.; Lee, J.-H.; Kim, T.; Ham, J.; Zheng, Z. N.; Lee, S. W. *C,N*-Palladacycles Containing N-Heterocyclic Carbene and Azido Ligand–Effective Catalysts for Suzuki–Miyaura Cross-Coupling Reactions. *Eur. J. Inorg. Chem.* **2012**, 6011. (c) Naziruddin, A. R.; Galstyan, A.; Iordache, A.; Daniliuc, C. G.; Strassert, C. A.; De Cola, L. Bidentate NHC^Pyrozolate Ligands in Luminescent Platinum(II) complexes *Dalton Trans*. **2015**, *44*, 8467.

(24) (a) Günay, M. E.; Özdemir, N.; Ulusoy, M.; Ucak, M.; Dincer, M.; Cetinkaya, B. The Influence of Moisture on Deprotonation Mode of Imidazolinium Chlorides with Palladacycle Acetate Dimer. *J. Organomet. Chem.* **2009**, *694*, 2179. (b) Hu, J. J.; Bai, S.-Q.; Yeh, H. H.; Young, D. J.; Chi, Y.; Hor, T. S. A. N-Heterocyclic Carbene Pt(II) Complexes from Caffeine: Synthesis, Structures and Photoluminescent Properties *Dalton Trans*. **2011**, *40*, 4402. (c) Xu, C.; Li, H.-M.; Xiao, Z.-Q.; Wang, Z.-Q.; Tang, S.-F.; Ji, B.-M.; Hao, X.-Q.; Song, M.-P. Cyclometalated Pd(II) and Ir(III) 2-(4-bromophenyl)-Pyridine Complexes with N-heterocyclic Carbenes (NHCs) and Acetylacetonate (acac): Synthesis, Structures, Luminescent Properties and Application in One-Pot Oxidation/Suzuki Coupling of Aryl Chlorides Containing Hydroxymethyl. *Dalton Trans*. **2014**, 43, 10235.

(25) (a) Hu, Y.; Li, L.; Shaw, A. P. Norton, J. R.; Sattler, W.; Rong, Y. Synthesis, Electrochemistry, and Reactivity of New Iridium(III) and Rhodium(III) Hydrides. *Organometallics* **2012**, *31*, 5058. (b) Keske, E. C.; Moore, B. D.; Zenkina, O. V.; Wang, R.; Schatte, G.; Crudden, C. M. Highly Selective Directed Arylation Reactions via Back-to-Back Dehydrogenative C–H Borylation/Arylation Reactions *Chem. Commun*. **2014**, *50*, 9883. (c) Hu, Y.; Norton, J. R. Kinetics and Thermodynamics of H−/H•/H+ Transfer from a Rhodium(III) Hydride *J. Am. Chem. Soc*. **2014**, *136*, 5938.

(26) Addison, A. W.; Rao, T. N.; Reedijk, J.; van Rijn, J.; Verschoor, G. C. Synthesis, Structure, and Spectroscopic Properties of Copper(II) Compounds containing Nitrogen-Sulphur Donor Ligands; the Crystal and Molecular Structure of Aqua[l,7-bis(N-methylbenzimidazol-2'-yl)-2,6-dithiaheptane]copper(ii) Perchlorate. *J. Chem. Soc., Dalton Trans*. **1984**, 1349.

(27) For the sake of comparison the inter–ring carbon–carbon bond lengths in biphenyl and 4,4'-bipyridyl (gas phase) are 1.49 and 1.465 Å and the torsion angles between the two rings are 40° and 37°, respectively. See CRC Handbook of Chemistry and Physics, 99th edition, 2018, CRC Press, ISBN 9781138561632.

(28) Grigg, R.; Mitchell, T. R. B.; Ramasubbu A. Rhodium-Catalysed Synthesis of Substituted Methylene Cyclopentanes. *Chem. Commun.* **1980**, 27.

(29) (a) Lim, Y.-G.; Kang, J.-B.; Kim, H. Regioselective Alkylation of 2-Phenylpyridines with Terminal Alkenes *via* C-H Bond Activation by a Rhodium Catalyst. *J. Chem. Soc., Perking Trans 1*, **1996**, 2201. (b) Yang, L.; Correia, C. A.; Li, C.-J. Rhodium-Catalyzed C–H Activation and Conjugate Addition under Mild Conditions. *Org. Biomol. Chem*. **2011**, *9*, 7176. (c) Schinkel, M.; Markek, I.; Ackermann, L. Carboxylate-Assisted Ruthenium(II)-Catalyzed Hydroarylations of Unactivated Alkenes through C–H Cleavage. *Angew. Chem. Int. Ed*. **2013**, *52*, 3977. (d) Zhou, B.; Ma, P.; Chen, H.; Wang, C. Amine-Accelerated Manganese-Catalyzed Aromatic C–H Conjugate Addition to α,β-unsaturated carbonyls. *Chem. Comun* **2014**, *50*, 14558. (e) Cheng, H.; Dong, W.; Dannenberg, C. A.; Dong, S.; Guo, Q.; Bolm, C. Ruthenium-Catalyzed Hydroarylations of Oxa- and Azabicyclic Alkenes. *ACS Catal* **2015**, *5*, 2770. (f) Zhang, M.; Hu, L.; Lang, Y.; Cao, Y., Huang, G. Mechanism and Origins of Regio- and Enantioselectivities of Iridium-Catalyzed Hydroarylation of Alkenyl Ethers. *J. Org. Chem.* **2018**, *83*, 2937.

(30) (a) Gonell, S.; Peris, E. Pyrene-Based Mono- and Di-N-Heterocyclic Carbene Ligand Complexes of Ruthenium for the Preparation of Mixed Arylated/Alkylated Arylpyridines. *ACS Catal*. **2014**, *4*, 2811. (b) Wu, S.; Huang, X.; Wu, W.; Li, P.; Fu, C.; Ma, S. A C-H Bond Activation-Based Catalytic Approach to Tetrasubstituted Chiral Allenes. *Nat. Commun*. **2015**, *6*, 7946. (c) Ghorai, D.; Dutta, C.; Choudhury. Switching of "Rollover Pathway" in Rhodium(III)-Catalyzed C−H Activation of Chelating Molecules. *ACS Catal*. **2016**, *6*, 709.

(31) (a) Kakiuchi, F.; Le Gendre, P.; Yamada, A.; Ohtaki, H. Murai, S. Atropselective Alkylation of Biaryl Compounds by Means of Transition Metal-Catalyzed C-H/Olefin Coupling. *Tetrahedron: Assimetry* **2000**, *11*, 2647. (b) Claiden, J.; Fletcher, S. P.; McDouall, J. J. W.; Rpwbottom, S. J. M. Controlling Axial Conformation in 2-Arylpyridines and 1-Arylisoquinolines: Application to the Asymmetric Synthesis of QUINAP by Dynamic Thermodynamic Resolution. *J. Am. Chem. Soc*. **2009**, *131*, 5331. (c) Newton, C. G.; Wang; S.-G.; Oliveira, C. C.; Carmer, N. Catalytic Enantioselective Transformations Involving C−H Bond Cleavage by Transition-Metal Complexes. *Chem. Rev*. **2017**, *117*, 8908.

(32) Kakiuchi, F.; Ohtaki, H.; Sonoda, M.; Chatani, N.; Murai S. Mechanistic Study of the $Ru(H)_2(CO)(PPh_3)_3$-Catalyzed Addition of C–H Bonds in Aromatic Esters to Olefins. *Chem. Lett.* **2001**, 918.

(33) Munárriz, J.; Rabuffetti, F. A.; Contrearas-García, J. Building Fluorinated Hybrid Crystals: Understanding the Role of Noncovalent Interactions. *Cryst. Growth Des.* **2018**, *18*, 6901.

(34) SAINT+: Area-Detector Integration Software, version 6.01; Bruker AXS: Madison, WI, 2001

(35) Sheldrick, G. M. SADABS program; University of Götingen: Göttingen, Germany, 1999.

(36) Sheldrick, G. M. SHELXS 97, Program for the Solution of Crystal Structure; University of Göttingen: Göttingen, Germany, 1997.

(37) Sheldrick, G. M. Crystal structure refinement with SHELXL. Acta Crystallogr., *Sect. C: Struct. Chem.* **2015**, *71*, 3.

(38) Farrugia, L. J. WinGX and ORTEP for Windows: an update. *J. Appl. Crystallogr*. **2012**, *45*, 849.

(39) Morse, P. M.; Spencer, M. O.; Wilson, S. R.; Girolami, G. S. *Organometallics* **1994**, *13*, 1646.

(40) Firsch, M. J.; Trucks, G. W.; Schlegel, H. B.; Scuseria, G. E.; Robb, M. A.; Cheeseman, J. R.; Scalmani, G.; Barone, V.; Mennucci, B.; Petersson, G. A.; Nakatsuji, H.; Caricato, M.; Li, X.; Hratchian, H. P.; Izmaylov, A. F.; Bloino, J.; Zheng, G.; Sonnenberg, J. L.; Hada, M.; Ehara, M.; Toyota, K.; Fukuda, R.; Hasegawa, J.; Ishida, M.; Nakajima, T.; Honda, Y.; Kitao, O.; Nakai, H.; Vreven, T.; Montgomery, Jr., J. A.; Peralta, J. E.; Ogliaro, F.; Bearpark, M.; Heyd, J. J.; Brothers, E.; Kudin, K. N.; Staroverov, V. N.; Kobayashi, R.; Normand, J.; Raghavachari, K.; Rendell, A.; Burant, J. C.; Iyengar, S. S.; Tomasi, J.; Cossi, M.; Rega, N.; Millam, J. M.; Klene, M.; Knox, J. E.; Cross, J. B.; Bakken, V.; Adamo, C.; Jaramillo, J.; Gomperts, R.; Stratmann, R. E.; Yazyev, O.; Austin, A. J.; Cammi, R.; Pomelli, C.; Ochterski, J. W.; Martin, R. L.; Morokuma, K.; Zakrzewski, V. G.; Voth, G. A.; Salvador, P.; Dannenberg, J. J.; Dapprich, S.; Daniels, A. D.; Farkas, Ö.; Foresman, J. B.; Ortiz, J. V.; Cioslowski, J.; Fox, D. J. *Gaussian 09, revision A.1*; Gaussian, Inc., Wallingford, CT, 2004.

(41) Zhao, Y.; Truhlar, D. G. The M06 Suite of Density Functionals for Main Group Thermochemistry, Thermochemical Kinetics, NonCcovalent Interactions, Excited States, and Transition Elements: Two New Functionals and Systematic Testing of Four M06-Class Functionals and 12 Other Functionals. *Theor. Chem. Account* **2008**, *120*, 215.

(42) Weigend F.; R. Ahlrichs, R. Balanced basis sets of split valence, triple zeta valence and quadruple zeta valence quality for H to Rn: Design and assessment of accuracy. *Phys. Chem. Chem. Phys.* **2005**, *7*, 3297.

(43) Marenich, A. V.; Cramer, C. J.; Truhlar, D. G. Universal Solvation Model Based on Solute Electron Density and on a Continuum Model of the Solvent Defined by the Bulk Dielectric Constant and Atomic Surface Tensions. *J. Phys. Chem. B* **2009**, 113, 6378.

(44) Bryantsev, V. S.; Diallo, M. S.; Goddard III, W. A. *J. Phys. Chem. B* **2008**, *112*, 9709.

(45) (a) Johnson, E. R.; Keinan, S.; Mori-Sanchez, P.; Contreras-Garcia, J.; Cohen, A. J.; Yang, W. *J. Am. Chem. Soc*. **2010**, *132*, 6498. (b) Contreras-Garcia, J.; Johnson, E. R.; Keinan, S.; Chaudret, R.; Piquemal, J.-P.; Beratan, D. N.; Yang, W. *J. Chem. Theory Comput.* **2011**, *7*, 625.